FINAL REPORT

U.S. DEPARTMENT OF ENERGY

ACTINIDE-SPECIFIC INTERFACIAL CHEMISTRY OF MONOLAYER COATED MESOPOROUS CERAMICS

Project Number -- 65370
(October 1998 to September 2001)

Principal Investigator

Dr. Glen E. Fryxell
Pacific Northwest National Laboratory
P.O. Box 999, MSIN K2-44
Richland, WA 99352
(509) 375-3856 (phone)
(509) 375-2186 (fax)
ge_fryxell@pnl.gov

Collaborators

Dr. Thomas S. Zemanian
PNNL
P.O. Box 999, MSIN P7-07
Richland, WA 99352
(509) 373-0344 (phone)
(509) 376-3002 (fax)
ts_zemanian@pnl.gov

Dr. Yuehe Lin
PNNL
P.O. Box 999, MSIN K8-93
Richland, WA 99352
(509) 376-0529 (phone)
(509) 376-5106 (fax)
yuehe.lin@pnl.gov

Hong Wu
PNNL
P.O. Box 999, MSIN P7-59
Richland, WA 99352
(509) 376-9446 (phone)
(509) 376-6767 (fax)
hong.wu@pnl.gov

Dr. Ken Kemner
Argonne National Laboratory
ER203 E-109
9700 S. Cass Ave.
Argonne, IL 60439
(630) 252-1163 (phone)
(630) 252-2959 (fax)
kemner@anl.gov

Dr. Shelly Kelly
Argonne National Laboratory
ER203 E-113
9700 S. Cass Ave.
Argonne, IL 60439
(630) 252-7376 (phone)
(630) 252-2959 (fax)
skelly@anl.gov

Professor K. N. Raymond
Department of Chemistry
Univ. of Cal. at Berkeley
Berkeley, CA 94720-1760
(510) 642-7219 (phone)
(510) 486-6145 (fax)
Raymond@socrates.berkeley.edu

TABLE OF CONTENTS

EXECUTIVE SUMMARY

The objective of this program was the design, synthesis and evaluation of high-efficiency, high-capacity sorbent materials capable of selectively sequestering actinides and other radionuclides from complex aqueous mixtures. Self-assembled monolayers on mesoporous supports (SAMMS) have proven to be a superior method of mercury and heavy metal sequestration, being orders of magnitude faster and more effective than existing mercury-scavenging methods. This project built upon the SAMMS concept and extended the interfacial chemistry of monolayer-coated mesoporous materials to the selective sequestration of actinides and cesium.

The high surface area of the mesoporous support (ca. 1000 m^2/g) coupled with the high population density of binding groups created by molecular self-assembly results in a very high loading capacity in the final SAMMS material. The rigid, open pore structure of the mesoporous support makes all of the interfacial binding sites available to solution borne species and allows for facile diffusion into the porous matrix, resulting in rapid sorption kinetics. The chemical specificity of a given type of SAMMS is governed by the monolayer interface. The ability to install chemically different monolayers, along with the ability to synthetically elaborate those monolayers post-installation, allows for a wide variety of binding chemistries to be installed, making the SAMMS concept easily tailored for a variety of environmental targets. This project focused on the design and installation of actinide-specific binding sites, as well as cesium-specific binding sites. These SAMMS materials were found to have high affinity for selectively sequestering their respective target species. In addition, sorption kinetics were generally found to be quite rapid. It was not uncommon for 99% of the target analyte to be sequestered within just a few minutes. Perhaps most importantly, the presence of competing ions (even

complexants like EDTA) had virtually no effect on the binding affinity of these SAMMS materials for the actinides and cesium. This work has clearly demonstrated that actinides and other radionuclides of interest to DOE can be selectively, efficiently and rapidly sequestered from complex mixtures by SAMMS.

Recently DOE has placed emphasis on the need to significantly reduce the volume of material put through the waste vitrification process. SAMMS, being a silica-based technology, is completely amenable to vitrification, and could be used to significantly reduce the volume of waste to be glassified since only the volume of the radionuclide-laden SAMMS would have to be vitrified and not the vast bulk of the waste. Due to the tendency of actinides to form insoluble hydroxides and polymeric oxide species at alkaline pHs, *any actinide separation method will require pH adjustment to a pH of less than 4 in order to be viable.* Such pH adjustment will approximately double the waste volume. However, even under the most conservative conditions SAMMS is employed in a solution/solid ratio of 100, thereby leading ultimately to reducing the volume of waste to be vitrified by *a factor of 50!* The likely HLW volume reduction is even greater since SAMMS can be effectively employed at solution/solids ratios of 500 to 1000, and in some cases even higher. As a result of this massive HLW volume reduction, the potential cost savings offered by SAMMS to the DOE clean-up effort is immense.

RESEARCH OBJECTIVES

Introduction

The objective of this program was to design, synthesize, and evaluate high-efficiency, high-capacity sorbent materials capable of selectively sequestering actinides and other radionuclides from complex aqueous mixtures. One of the central goals of this project was to understand the fundamental interfacial science required to develop novel mesoporous materials coated with organized monolayers of rationally designed ligands, custom-tailored for binding specific actinide cations. This capability addresses waste management by separation of actinides, a central concern of high-level waste (HLW) management at several DOE sites.

Problem Statement

The need exists in the management of DOE's HLW to be able to selectively and completely remove the radionuclides so that HLW volume can be minimized and the nonradioactive components can be segregated and disposed of as low-level waste (LLW), thus substantially reducing remediation costs. In addition, the short-term risk assessment for tank closure requires a complete and accurate accounting of actinide speciation. This can be done either via direct separation or by concentration of low-level actinides and subsequent separation from the matrix. Isolation of individual actinides such as americium is a key parameter in the risk assessment necessary for tank closure. There are currently no methods available to distinguish or separate americium from plutonium at extremely low concentrations. This is essential information for the short-term risk assessment for HLW tank closure.

These needs dictate the development of selective and efficient separation of actinides from complex waste streams so as to minimize HLW volume, reduce waste management costs, and enhance long-term stability of the HLW form. Recently DOE has placed emphasis on the need to significantly reduce the volume of material put through the vitrification process. Thus, selective separation of the actinides and radiocesium from tank waste forms a critical need for this waste management strategy.

Strategy

PNNL has developed self-assembled monolayers on mesoporous supports (SAMMS) as a superior method of mercury and heavy metal sequestration, proving to be orders of magnitude faster and more effective than existing mercury-scavenging methods. [1-7] This project built upon the SAMMS concept and extended the interfacial chemistry of monolayer-coated mesoporous materials to study the requirements of selectively binding of actinides and cesium.

The highly ordered nanostructure of SAMMS is the culmination of three successive generations of molecular self-assembly. The first generation is the aggregation of the surfactant molecules to create the micelle template; the second is the aggregation of the silicate coated micelles into the mesostructured greenbody, and the third is the self-assembly of the silane molecules into an ordered monolayer structure across the pore interface. This functionalized hexagonal honeycomb structure is a powerful foundation upon which to build an environmental sorbent material.

The SAMMS concept allows for significant freedom in the design and synthesis of tailored materials for actinide separation. The mesoporous ceramic synthesis is quite general and can be used to prepare a variety of high surface area ceramic oxide supports that are stable in different environments (acidic, corrosive, oxidizing, etc.). The high surface area of the

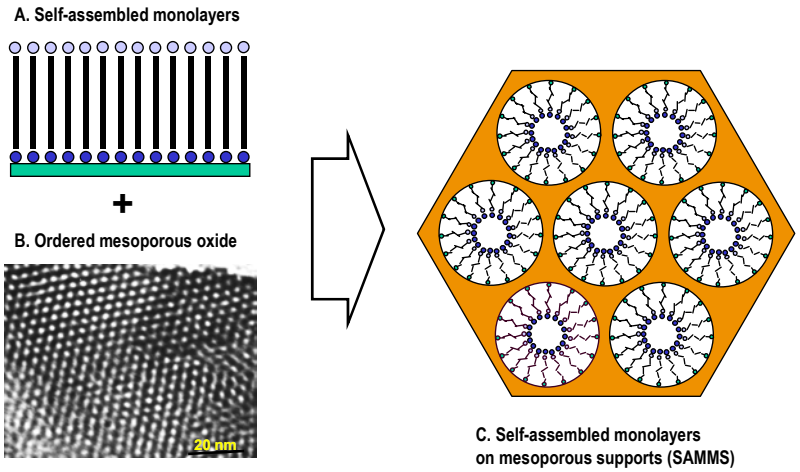

Figure 1. The origins of SAMMS

mesoporous support (ca. 1000 m^2/g) coupled with the high population density of binding groups creates a high loading capacity in the final SAMMS material. The rigid, open pore structure of the mesoporous support makes all of the interfacial binding sites available to solution borne species and allows for facile diffusion into the porous matrix, resulting in rapid sorption kinetics. The chemical specificity of a given type of SAMMS is governed by the monolayer interface. The ability to install chemically different monolayers, along with the ability to synthetically elaborate those monolayers post-installation, allows for a wide variety of binding chemistries to be installed, making the SAMMS concept easily tailored for a variety of environmental targets (Pu, Cs, TcO_4, etc.). SAMMS, being a silica-based technology, would be readily incorporated into a vitrification process stream. This would reduce the volume of waste needing vitrification by orders of magnitude since only the volume of the radionuclide-laden SAMMS would have to be vitrified and not the bulk of the waste.

METHODS AND RESULTS

Lanthanide Model Studies

Initial testing used lanthanides to mimic actinides to perform preliminary screening more cost-effectively by avoiding radioactive materials. La (III) was chosen as a "light" lanthanide, with an ionic radius very similar to Th (IV) (see Table 2). Nd (III) was chosen as a "typical" lanthanide, with an ionic radius similar to many of the actinide cations. Eu (III) was chosen since it has been used in the past as an Am (III) mimic, and because it is very similar in size to U (IV), Np (IV) and Pu (IV), the actinides of particular interest in the DOE clean-up. Lastly, Lu (III) was included in these studies as a cation with an ionic radius in between those typically

found for the rare earth cations and those found for the transition metal cations, typical of those late in the lanthanide series.

We employed three related synthetic pathways to prepare our functionalized SAMMS materials, exemplifying the versatility of our convergent SAMMS synthesis. Glycinyl-urea SAMMS were prepared by treating an isocyanate terminated silane with a triethylamine buffered solution of glycine. This approach tethers the acid to the silane *via* a urea linkage. (see Figure 2) In this fashion, we obtained a glycine terminated SAMMS material with a surface coverage of approximately 4.0 silanes/nm^2 (as determined by solid-state ^{29}Si NMR).

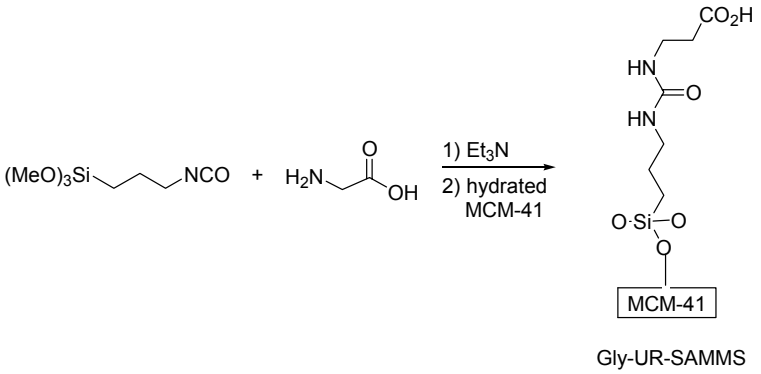

Figure 2. Preparation of Glycinyl-urea (Gly-UR) SAMMS

The second of our strategies is exemplified by the incorporation of the salicylate ligand *via* an amide linkage to commercially available aminopropylsiloxane (APS), accomplished by activating the carboxylate with carbonyl diimidazole (see Figure 3). All attempts to effect this amidation *via* the corresponding methyl and ethyl esters failed. The CDI amidation reaction was followed immediately by deposition in freshly hydrated MCM-41. This protocol resulted in the deposition of 1.1 silanes/nm^2, which is the expected level of coverage for an aromatic terminated silane of this bulk. This strategy was also used to make the *p*-NO_2 analog, and other related aromatic interfaces, resulting in similar coverage densities.

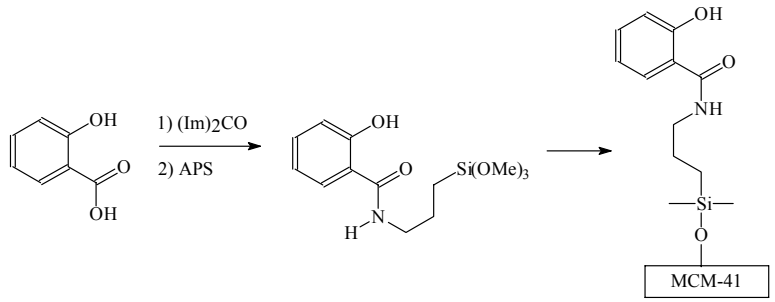

Figure 3. Pre-assembly of the salicylamide ligand

The HOPO ligands were incorporated using a variation of this carboxylate activation scheme. In this case, carbonyl activation was accomplished using the thiaz group, carried out on the benzyl protected HOPO acid (see Figure 4). The activated carboxylate was then treated with APS as before and deposited in similar fashion. After deposition, the benzyl protecting groups were removed *via* treatment with 10% HBr in glacial acetic acid, affording the desired HOPO

interface. This procedure resulted in deposition of 0.5-1.0 silanes/nm^2 (the slightly lower silane density is the result of the steric bulk of the benzyl protecting groups).

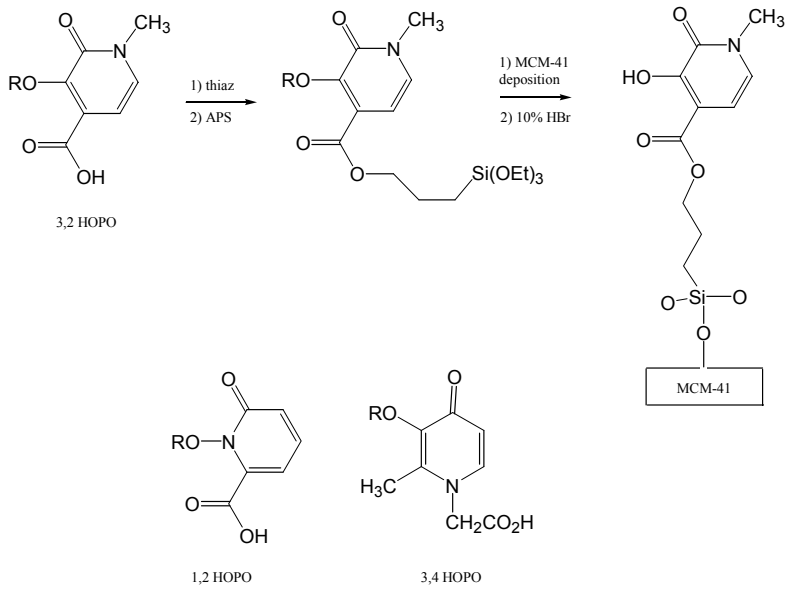

Figure 4. Preparation of HOPO SAMMS *via* thiaz activation

The third synthetic route was used to prepare the phosphonate SAMMS, and involved displacement of trifluoroethanol from the corresponding ester, as shown in Figure 5.

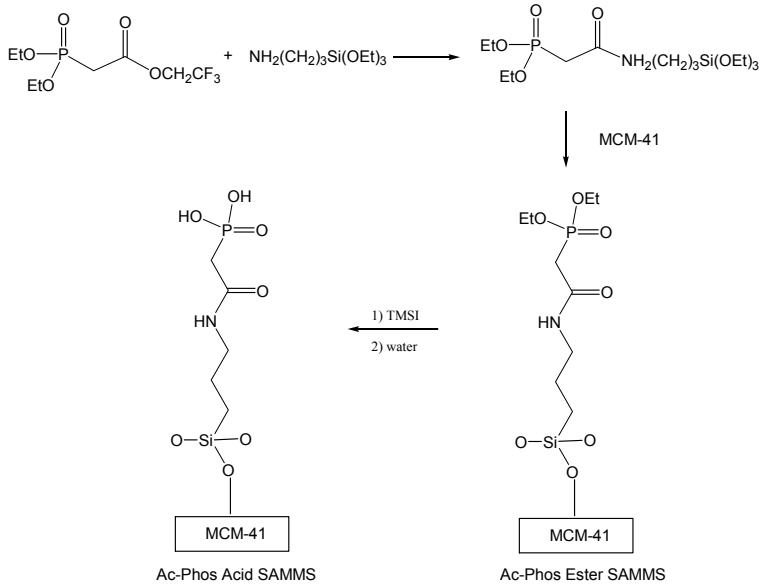

Figure 5. Preparation of phosphonic acid SAMMS

Distribution Coefficient Measurements. The lanthanide and actinide target species commonly form insoluble hydroxides or polymeric oxides under alkaline conditions, so our

lanthanide binding studies were performed over a pH range of 1.0 to 6.5. Cation binding is an equilibrium process and can be influenced by the stoichiometric ratio of binding sites to solution cation content. The solution/solids ratio employed in these experiments was typically 200, but was also studied in a range from 100 to 1000. In order to insure that all distribution coefficients reflected genuine equilibrium conditions, contact times were several hours (typically 2-4; as will be shown later, equilibrium under these conditions is reached within only a few minutes).

$$K_d = \frac{(C_o - C_f)}{C_f} * \frac{V}{M}$$

The distribution coefficients (K_d) are simply a mass-weighted partition coefficient between the aqueous supernatant phase and SAMMS solid phase, and these results are summarized in Table 1. The higher the K_d value, the more effective the sorbent material is at sequestering the target species. Kd's above 500 are considered good, those above 5,000 are considered excellent and Kd's in excess of 50,000 are considered outstanding. As can be seen from the data, most of these SAMMS were very effective at removing the lanthanides at the higher pH's, with attenuating affinity as the pH dropped.

Table 1. Lanthanide Distribution Coefficients for Salicylamide SAMMS

Lanthanide Kd's for Sal-SAMMS				
Metal	**pH=1**	**pH=2.5**	**pH=4.5**	**pH=6.5**
La	0	0	17	7867
Nd	0	0	18	>100,000
Eu	0	129	17109	47950
Lu	6	2	20	>100,000

0.1M NaNO3, 2ppm La, 10 mL, 0.100g SAMMS

One of the simplest and most direct entries into a synergistic ligand field is provided by the salicylamide ligand due to the combination of the resonance stabilized phenolic OH group and the adjacent amide carbonyl group. Salicylamide-based ligands have been used to chelate a wide variety of metal cations [8], and recently salicylamide based ligand systems have been very elegantly employed to create elaborate supermolecular complexes [9]. Sal- SAMMS was found to be an effective method of sequestering lanthanide cations, but only at the higher pH's. In addition, it showed a distinct preference for binding the smaller cations (*e.g.* Lu and Eu), as opposed to the larger La (III) cation. This is not surprising given that the salicylamide ligand forms a rigid, 6-membered ring chelate, and thus has a limited "cavity" in which to bind the cation. The pH limitation found with this sorbent was initially thought to arise from the modest acidity of the phenolic hydroxyl group. As a means of testing this hypothesis, we also prepared and studied the 5-nitro analog, as well as phthalamide SAMMS (the corresponding ortho carboxylic acid). Neither one of these more acidic ligands demonstrated any notable improvement over the original Sal-SAMMS.

Table 2. Lanthanide Distribution Coefficients for Glycinyl-Urea SAMMS

Lanthanide Kd's for Gly-UR-SAMMS				
Metal	**pH=1**	**pH=2.5**	**pH=4.5**	**pH=6.5**
La	3	79	18150	73680
Nd	0	107	18490	94000
Eu	0	129	17109	47950
Lu	2	73	12979	40889

0.1 M NaNO3, 0.05M NaOAc,
10mL 2 ppm La solution, 0.05g SAMMS

The rigid nature of the benzene ring precludes coplanar chelation of the metal cation if the ionic radius of the cation is large (as with the early lanthanides and low oxidation state actinides). Thus, we chose to explore the conformationally more flexible sp^3 hybridized ligand systems, in conjunction with 7-membered chelates. Gly-UR SAMMS were found to have broad-scale binding affinity for all of the lanthanides studied. In addition, they were found to have a broader pH window, effectively binding the target lanthanides to below a pH of 4 (see Table 2). The conformationally flexible Gly-UR SAMMS were found to bind the large and small lanthanide cations with equal ease.

Ac-Phos ester SAMMS have both the carbonyl amide and the P=O ester ligands incorporated as a part of the monolayer interface. Both of these groups activate the central enolizable methylene, creating the protic portion of the ligand (similar to the classic acetonylacetonate, or acac ligand). The ambiphilic wettability of the phosphonate ester interface makes these SAMMS materials particularly well-suited for sequestering species from non-aqueous waste streams (*e.g*. oils, cutting fluids, solvents, *etc*.).

Table 3. Lanthanide Distribution Coefficients for Ac-Phos Ester SAMMS.

Lanthanide Kd's for AcPhos ester SAMMS				
Metal	**pH=1**	**pH=2.5**	**pH=4.5**	**pH=6.5**
La	139	1779	49050	63233
Nd	283	4857	73466	107300
Eu	593	14881	129600	182100
Lu	215	4888	98200	199800

0.1M NaNO3, 2ppm La, 10 mL, 0.05g SAMMS

Ac-Phos ester SAMMS are particularly good at sequestering the target lanthanides, and in fact are able to do so down to a pH of approximately 2. Once again, the 6-membered ring chelate favors the smaller lanthanide cations (*e.g.* Lu and Eu) relative to the larger La (III). While Ac-Phos ester SAMMS is an effective sorbent for the lanthanides, it also shows a modest affinity for certain transition metals, particularly Fe(III), which may limit its utility as an environmental sorbent material since Fe will undoubtedly be present in the environment at higher levels than the target species.

The homologation of Ac-Phos ester SAMMS to form Prop-Phos ester SAMMS does two things. First, it significantly attenuates the acidity of the enolizable methylene, and secondly it increases the chelate ring size to 7. In a series of neutral diamide ligands designed as solution extractants, 7-membered chelates are known to effectively ligate the lanthanide cations [10]. In any event, Prop-Phos ester SAMMS shows very little affinity for lanthanide cations, suggesting

that perhaps the primary diving force for the sequestration observed with the Ac-Phos ester SAMMS is enolization of the active methylene, and formation of the neutral adduct.

Table 4. Lanthanide Distribution Coefficients for Prop-Phos Ester SAMMS.

Prop-Phos ester SAMMS Kd study				
Metal	**pH=1**	**pH=2.5**	**pH=4.5**	**pH=6.5**
La	8	1	11	22
Eu	0	7	1	51

0.1M NaNO3, 2ppm La, 10 mL, 0.05g SAMMS

The phosphonate esters were cleaved using trimethylsilyl iodide in anhydrous acetonitrile, followed by hydrolysis to afford the corresponding phosphonic acids. Both of these new SAMMS were found to be exceptionally good lanthanide scavengers above a pH range of 2, but displayed lesser affinities under strongly acidic conditions, as shown in the K_d data below. At pHs of 4 and above, distribution coefficients of 300,000 or more were commonly observed for the phosphonic acid SAMMS. For a solution to solids ratio of 200, this indicates that more than 99.9% of the target analyte is captured in the SAMMS phase.

Table 5. Lanthanide Distribution Coefficients for Ac-Phos Acid SAMMS.

pH	Kd (La)	Kd (Nd)	Kd (Eu)	Kd (Lu)
3M HNO3	135	134	140	113
1M HNO3	140	154	200	153
1.7	62120	37925	35444	86150
4	304600	73200	77800	338400
5.7	344200	178600	120000	379800

The entire range of ionic radii are bound effectively by the Ac-Phos acid SAMMS. The Ac-Phos acid SAMMS appears to be very egalitarian in its taste for the lanthanide cations.

The Prop-Phos acid SAMMS also displays excellent affinity for the lanthanide cations down to a pH of about 2. The acid form of Prop-Phos SAMMS clearly has a significantly higher affinity for the lanthanide cations in the Prop-Phos than does the ester form. At a pH of 2, the Prop-Phos acid SAMMS seems to show an interesting selectivity for the smaller Lu cation. The source of this selectivity is not clear at this point.

Table 6. Lanthanide Distribution Coefficients for Prop-Phos Acid SAMMS

pH	Kd (La)	Kd (Nd)	Kd (Eu)	Kd (Lu)
3M HNO3	11	7	0	0
1MHNO3	4	1	0	0
2	2047	11968	5994	405800
4	332200	330200	187500	397600
6	381400	190840	184800	390200

EXAFS Measurements. Detailed EXAFS analysis of the Eu (III) adduct of Sal-SAMMS revealed an average Eu-O coordination number of 8 ± 1.2, a Eu-O radial distance of 2.40 ± 0.015

Å, and an XAFS Debye-Waller term of 0.0145 ± 0.0025 $Å^{-2}$. These results are consistent with the Eu (III) cation being 8-coordinate (not unusual for the lanthanides), in either a cubic or distorted square antiprism geometry. Taking into account the geometric considerations of the monolayer interface, a distorted square antiprism is the most likely bonding geometry for this complex.

These EXAFS results support the conclusion that the close proximity of the ligands in the monolayer interface allow for multiple ligands to interact with a single metal cation. In this case we observe a 4 to 1 ligand:metal interaction, which clearly contributes to enhancing the binding affinity between a given ligand and metal cation.

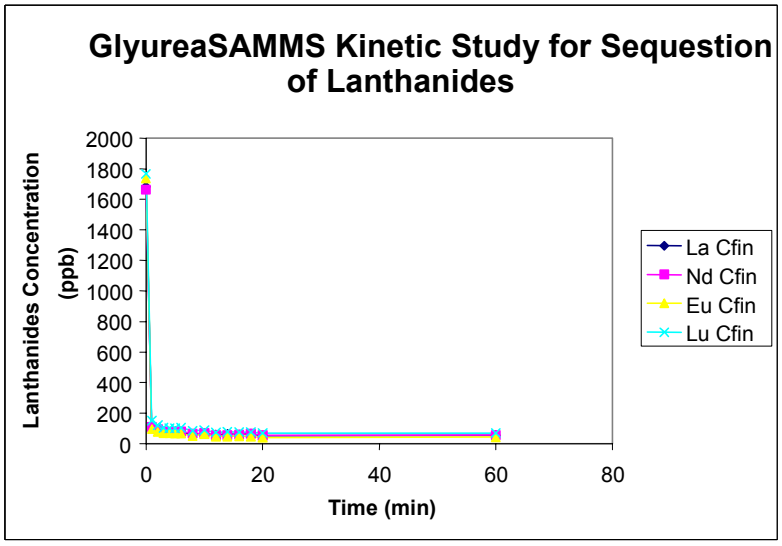

Figure 6. Kinetics of lanthanide sequestration using Gly-UR SAMMS

Lanthanide Sorption Kinetics. Sorption kinetics play an important role in the efficiency and cost of the field deployment of a sorbent system. The lanthanide sorption kinetics of Gly-UR SAMMS were explored using 4 different lanthanides. As can be seen from the data summarized in Figure 6, equilibrium was reached in less than one minute under these conditions. Ac-Phos and Prop-Phos acid SAMMS kinetics were virtually identical, once again with equilibrium being reached in less than one minute.

The lanthanide binding kinetics of SAMMS in an actual field deployment will be dependent on cation concentration, solution/solids ratio, viscosity, mixing efficiency, etc., but these results clearly demonstrate that diffusion into and out of the mesoporous matrix and the binding chemistry at the monolayer interface is an inherently facile process. It is worth noting that these sorption kinetics are quite similar to those obtained in our previous mercury scavenging studies [3, 6].

Competition Studies. For a sorbent material to have any value in the field, it must exhibit at least modest selectivity for the target species, and not be saturated with common, ubiquitous competing ions, leaving little or no activity for the target species. Thus, we undertook a study of the effects of competing cations on Nd binding for both Gly-UR and Ac-Phos ester SAMMS. The results of these competition studies are summarized in Tables 7-10. Very little competition was observed when using the Ac-Phos ester SAMMS, and that was limited to modest

competition from Fe. The Gly-UR SAMMS demonstrated no competing affinity for the transition metals.

Table 7. Competition Studies using Glycinyl Urea SAMMS and Nd (III)

competitor (ppm)	Nd_{ini} ppb	Nd_{fin} ppb	Kd (Nd)
none	1843	12	30,517
Fe=20	1807	12	29,917
Ni=20	1774	12	29,367
Cu=20	1776	11	32,091
Zn=20	1787	10	35,540
K=20	1798	10	35,760
Ca=150	1720	11	31,073
mixture	1680	10	33,400

0.1M NaNO3, pH=5.0, 0.05g SAMMS

Table 8. Competition Experiments using Ac-Phos ester SAMMS and Nd(III)

sample	element	C_{ini} ppb	C_{fin} ppb	Kd (Nd)
1	Nd	1725	26	13,069
2	Nd	1695	35	9486
	Fe	19090	814	4490
3	Nd	1680	26	12,723
	Ni	19950	16750	38
4	Nd	1636	21	15,381
	Cu	19430	14270	72
5	Nd	1529	30	9993
	Zn	17420	14240	45
6	Nd	1521	19	15,810
	K	15450	14840	8
7	Nd	1518	43	6860
	Ca	141400	133400	12
8	Nd	1402	53	5091
	Fe	17500	692	4858
	Ni	18510	18090	5
	Cu	18630	16150	31
	Zn	16690	14700	27
	K	14770	14290	7
	Ca	133300	123600	16

0.1M NaNO3, pH=5.0, 0.05g SAMMS

In studies of the Ac-Phos acid SAMMS, only modest competiton was observed from Fe, Cu and Zn cations. The affinity for the lanthanide model systems remained high in spite of this modest compeition.

The modest competition from Fe(III) observed with the Ac-Phos ester SAMMS and Ac-Phos acid SAMMS can be explained by the ligand forming a 6-membered ring chelate with the metal cation, which is widely recognized as a favorable chelation mode for transition metals.

Thus, it is not surprising that this ligand shows a modest affinity for the smaller and more acidic Fe(III). In the case of the Gly-UR, which forms a 7-membered ring chelate with a metal cation, there was virtually no competition observed with any of the competing ions studied. This is consistent with the ionic radius arguments presented above – the larger lanthanide cations coordinate nicely in the larger ligand cavity, but the smaller transition metals suffer from something of a stereochemical mismatch.

Table 9. Competition Studies using Ac-Phos ester SAMMS and Eu(III)

sample	element	C_{ini} ppb	C_{fin} ppb	Kd (Eu)
1	Eu	2070	5	82,600
2	Eu	2160	940	260
	Fe	21400	2130	1,809
3	Eu	2130	3	141,800
	Ni	19770	17660	24
4	Eu	2110	5	84,200
	Cu	19770	15920	48
5	Eu	2050	4	102,300
	Zn	20300	18940	14
6	Eu	2150	2	214,800
	K	21900	19360	26
7	Eu	2090	8	52,050
	Ca	137200	128100	14
8	Eu	2060	1088	179
	Fe	20300	2450	1,457
	Ni	18240	18390	0
	Cu	19590	21520	0
	Zn	20050	20200	0
	K	20080	20500	0
	Ca	136500	135800	1

10 mL 0.1M NaNO3, 0.05M NaAc, pH=2.0, 0.05g SAMMS

Table 10. Competition Studies using Ac-Phos Acid SAMMS and Lanthanides

sample	element	Cini ppb	Cfin ppb	Kd
	La	2080	1	415800
	Nd	2110	12	34967
	Eu	2200	9	48689
1	Lu	2220	8	55300
	La	1911	1	382000
	Nd	1980	5	79000
	Eu	2170	2	216800
	Lu	2160	2	215800
2	Fe	21500	325	13031
	La	1743	1	348400
	Nd	1811	5	72240
	Eu	2040	6	67800
	Lu	2030	5	81000
3	Ni	19590	5670	491
	La	2035	1	406800
	Nd	1997	17	23298
	Eu	1990	5	79400
	Lu	1976	4	98600
4	Cu	19580	851	4402
	La	1978	1	395300
	Nd	1925	17	22449
	Eu	1960	5	78200
	Lu	1950	4	97300
5	Zn	19830	2130	1662
	La	1986	1	397000
	Nd	2040	9	45133
	Eu	2210	8	55050
	Lu	2200	8	54800
6	K	22600	23200	0
	La	1881	1	376050
	Nd	1844	15	24386
	Eu	1928	12	31933
	Lu	1885	6	62633
7	Ca	21800	21400	4
	La	2133	10	42452
	Nd	2054	17	23966
	Eu	2108	13	32231
	Lu	2056	7	58543
	Fe	20400	837	4675
	Ni	19910	21000	0
	Cu	20080	16320	46
	Zn	21100	21200	0
	K	20110	23800	0
8	Ca	23600	24800	0

0.1M NaNO3, 0.05M NaAc, pH=4.0, 0.05g SAMMS

Regeneration Studies. The ability to regenerate any sorbent material is a key factor in determining life cycle costs and field application strategy. The fact that all of these SAMMS show lesser K_d's at lower pHs suggests that it might be possible to strip the lanthanides from the SAMMS phase with an acid wash. In order to test this, we regenerated the Gly-UR SAMMS by stripping the sorbed europium with an acid wash (0.5 M HCl), and then re-exposing the SAMMS to fresh europium solution and re-measured the sorption affinity. Repeating this cycle 10 times revealed no loss in binding affinity (see Table 11). Clearly, regeneration of SAMMS is both easy and effective, making recycling of these nanostructured sorbent materials a viable option in their deployment.

Table 11. Acid Regeneration of Glycinylurea SAMMS and Eu (III) binding affinity

Cycle	Cini ppb	Cfin ppb	Kd
1	1708	76	4295
2	1800	73	4732
3	1922	88	4168
4	1826	74	4735
5	1730	57	5870
6	1892	50	7368
7	1870	50	7280
8	1742	49	6910
9	1814	67	5215
10	1438	43	6488

pH = 4

Actinide Studies

Distribution Coefficient Measurements. Much has been learned in terms of metal-ligand interactions from actinide solvent extraction studies, as well as those studies aimed at designing ligands to remove actinides from biological systems. As discussed earlier, the key lessons arising from these studies are that the actinide cations are hard Lewis acids, that are considerably larger than the typical transition metal cation and that ligand synergy is an important attribute to design into a ligand field. Noteworthy examples of how these concepts have been joined into powerful rare earth ligand systems include the HOPO and DFO chelators [11], and the CMPO extractants [12]. The lanthanide model studies suggested that SAMMS are a viable method for sequestering actinides, and that the synergistic ligand field concept outlined above is indeed valid at the monolayer interface inside a mesoporous matrix.

The data in Table 12 reveal that the carboxylic acid SAMMS do indeed bind actinides effectively (especially the Gly-UR SAMMS), but once again the binding is heavily dependent on pH, with the better binding efficiency at higher pH's.

Table 12. Actinide Distribution Coefficient values for the carboxylic acid SAMMS

Actinide	pH	Kd	Kd
		Phthal-SAMMS	Gly-UR SAMMS
Am(III)	0.78	0	0
	1.9	0	1
	4.26	51	91739
	5.24	1406	242439
Pu(IV)	0.66	0	157
	1.05	46	5091
	2.08	8965	45,000
Np(V)	0.72	0	0
	1.55	0	0
	3.68	0	86
	4.73	0	200
U(VI)	0.7	57	156
	2.36	125	11994
	4.55	2825	161246
Th(IV)	0.76	34	903
	2.43	1981	90758

[Ac] = 2000 cpm/mL
0.1M $NaNO_3$
0.10 g SAMMS in 10 mL

Studies with the carboxylic acid SAMMS revealed that they were limited in terms of their effective pH range, with their binding affinities for the actinides dropping off below a pH of 2. This is not unexpected because of the basicity of the carboxylate ligand. However, as a result of the ubiquitous nature and low cost associated with carboxylate ligands (*e.g.* glycine derivatives) and the fact that they function well in the pH range of 2-4, these ligands may offer a cost-effective compromise for treating HLW.

A pair of CMPO analogs were studied. The Ac-Phos ester was found to be effective for all of the actinides studied except for the difficult to bind Np(V). In contrast, the Prop-Phos ester was found to be selective for Pu(IV), and especially so at low pH's. In fact, as is apparent from the data below, Pu(IV) and Am(III) are easily and almost quantitatively separated by a single simple treatment with Prop-Phos ester SAMMS, as shown below. Finding such a separation method was one of the goals of this project.

Table 13. Actinide Distribution Coefficients for the Phosphonate Ester SAMMS

Actinide	pH	Kd	Kd
		Ac-Phos SAMMS	Prop-Phos SAMMS
		diethyl ester	diethyl ester
Am(III)	0.78	595	0
	1.9	3912	0
	4.26	206111	33
	5.24	464806	48
Pu(IV)	0.66	93868	61393
	1.05	72433	66338
	2.08	52089	35,640
Np(V)	0.72	60	0
	1.55	55	0
	3.68	43	0
	4.73	147	0
U(VI)	0.7	25560	172
	2.36	30819	1420
	4.55	23827	11548
Th(IV)	0.76	22638	20909
	2.43	12781	31441

[Ac] = 2000 cpm/mL
0.1M NaNO3
0.20 g SAMMS in 10 mL

Table 14. Pu/Am Separation using Prop-Phos Ester SAMMS.

Pu(IV)/Am(III) Separation using Prop-Phos SAMMS (ester form)

Solution	Radioisotope	pH	% removal
0.1 M NaNO3	Pu(IV)	0.88	99
	Am(III)	0.88	0
	Pu(IV)	1.6	96
	Am(III)	1.6	1
2.0M NaNO3	Pu(IV)	0.7	98
	Am(III)	0.7	0
	Pu(IV)	1.5	88
	Am(III)	1.5	9

Initial activity = approximately 2100 cpm/mL of each actinide
0.02 g SAMMS, 10 mL solution

Pu(IV) and Am(III) Separation. A mixture of Pu (IV) and Am (III) were shaken with a sample of Prop-Phos ester SAMMS, the mixture was filtered and the separate phases subjected to analysis. These experiments were repeated at different pH's and nitrate concentrations to explore the impact that these variables had on the separation. In 3 of the 4 test cases, Pu

recovery in the solid SAMMS phase was virtually quantitative, and almost all of the Am was left in the supernatant solution. This separation is particularly effective at the lower pHs. This is clearly a very facile separation method.

Kinetics Studies

The sorption kinetics for Pu (IV) were studied for the Ac-Phos and Prop-Phos SAMMS, in both the ester and acid forms. The data shown below for the phosphonate ester SAMMS binding of Pu(IV) indicates that equilibrium isn't reached for 1-2 hours. This is notably slower than for the lanthanide binding studies described earlier which used SAMMS terminated with protic ligands. We feel that this is due to the fact that Pu(IV) is known to form strong complexes with nitrate anion, and the neutral Ac-Phos ligand has trouble competing with nitrate anion for the Pu(IV) cation, making the initial binding interaction slow. However, once bound by the first Ac-Phos ligand, the high local concentration and close proximity of the ligands allows for multiligand chelation of the Pu(IV) cation, and hence a strong binding affinity overall.

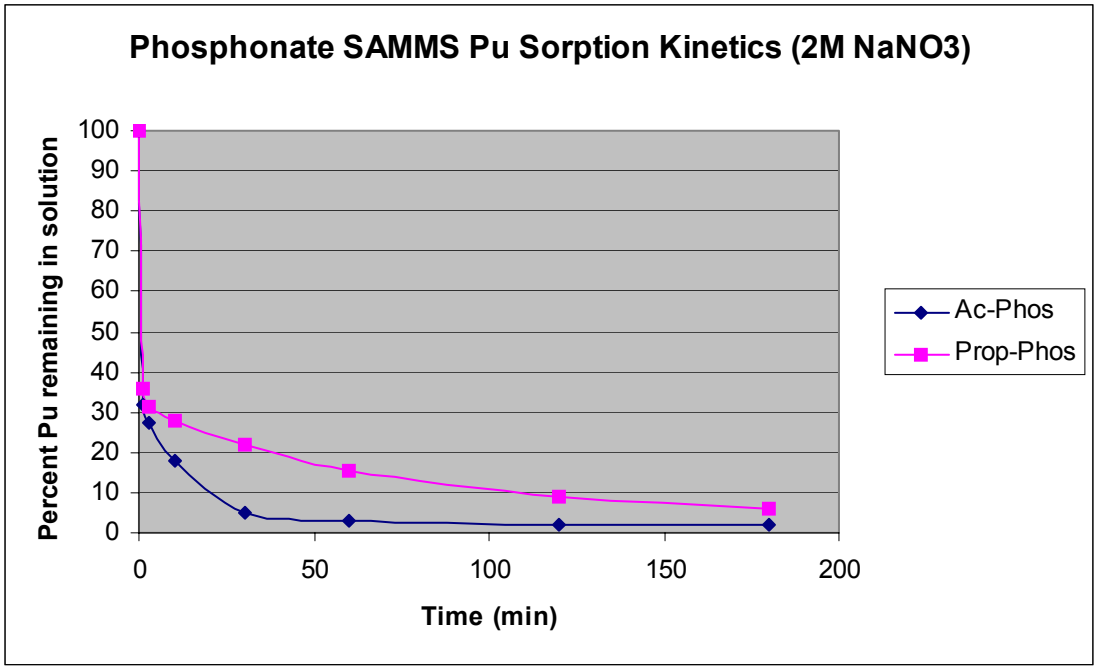

Figure 7. Kinetics of Pu (IV) sorption using the phosphonate ester SAMMS.

In contrast, the binding kinetics of the phosphonic acid SAMMS was found to be exceptionally rapid, and virtually identical to those observed for the lanthanide model systems using protic ligands. Once again, it is apparent that diffusion into the mesoporous matrix is not a significant kinetic limitation.

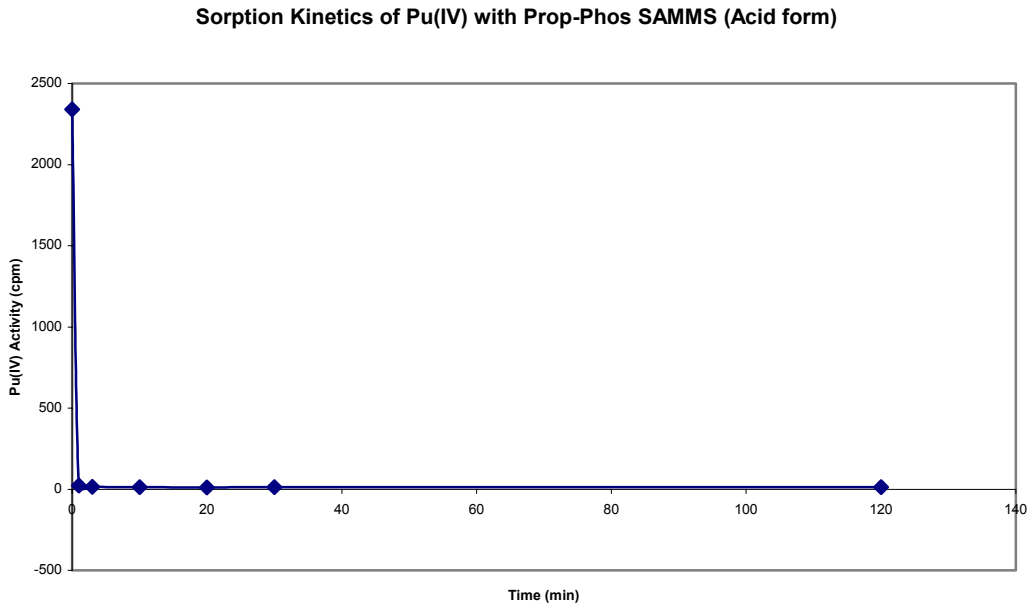

Figure 8. Sorption Kinetics of Pu (VI) using Prop-Phos Acid SAMMS

Nitrate Dependence. It became apparent during the course of these studies that the Kd values for Pu with various SAMMS tended to vary somewhat depending on the nitrate concentration of the solution matrix. Thus, we explored this effect in detail. The data are summarized in Figure 9. As can be seen, the Kd values tend to be quite high at low nitrate concentrations, and decrease with increasing nitrate concentration up to approximately 1 M nitrate, beyond which the Kd values level off with no further attenuation. It has been known for some time that Pu forms strong complexes with nitrate anion (citation 56 in the EMSP renewal 01), and that affinity is thought to be the source of this competition. While this is indeed a concern in terms of the ultimate implementation of SAMMS for Pu separations, it must be noted that the effect does level off above 1 M nitrate and the Kd values are still on the order of 10,000 to 20,000, making this a strong separations method in spite of this effect

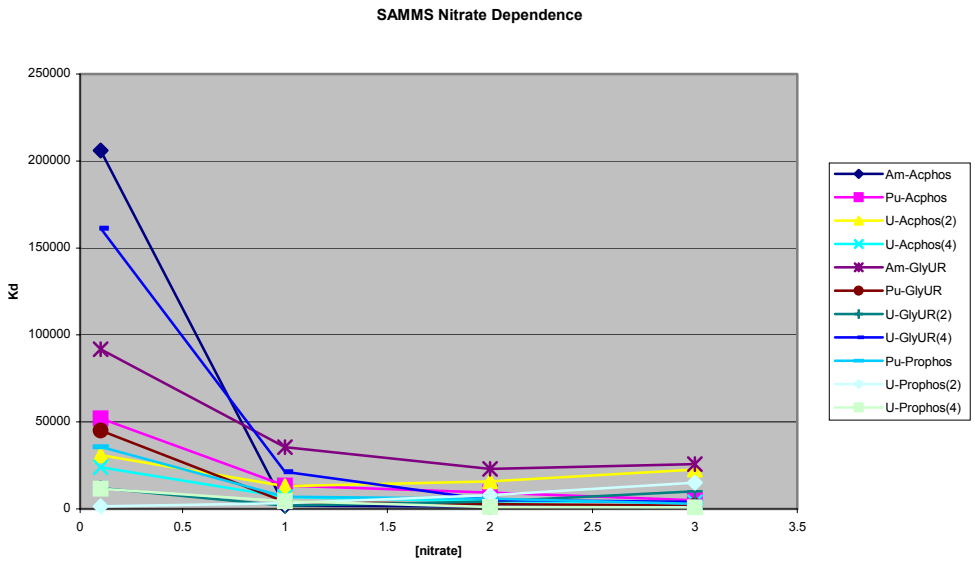

Figure 9. Actinide SAMMS Distribution Coefficient Dependence on Nitrate Concentration

Table 15. Pu (IV) Competition Studies with Phosphonate Ester SAMMS

Competitor	Concentration	Kd (Pu) Ac-Phos diethyl ester	Kd (Pu) Prop-Phos diethyl ester
None		10865	4178
Fe(III)	100 ppm	6029	2870
Al(III)	100 ppm	9923	4015
Zr(IV)	100 ppm	9691	562
Ni(II)	100 ppm	11172	4632
Ca(II)	100 ppm	10037	4051
Mn(II)	100 ppm	8363	2190
Mo(VI)	100 ppm	8611	4822
Cu(II)	100 ppm	9299	4107
Pb(II)	100 ppm	11911	4175
Cr(III)	100 ppm	11326	4031
Hg(II)	100 ppm	10089	4195
Phosphate	0.01M	10457	3746
Sulfate	0.01M	10610	3415
EDTA	0.01M	59	4
Citrate	0.01M	11583	2236

[Pu] = 2000 cpm/mL
1M $NaNO_3$
0.1 M HNO_3

Competition Studies. Competition studies carried out with the phosphonate ester SAMMS reveal the same competition from ferric ion as observed with the lanthanide model systems (see Table 15). In addition, there is an interesting anionic competition noted for both Pu

(with zirconate) and U (with molybdate). It is worth noting that the lanthanide studies suggested that Prop-Phos ester SAMMS would be a poor actinide scavenger, and that is indeed the case for U (VI), however the Pu (IV) affinity is still moderately high, indicating the limitations of using lanthanides as model systems for the actinides.

In the Pu (IV) competition studies, a severe competitive interaction observed was with EDTA, which seriously attenuated the binding affinity of both the Ac-Phos and Prop-Phos ester SAMMS.

A similar series of experiments was carried out for U (VI), and once again it was found that Fe (III) offered some significant competition (see Table 16). In addition, modest competition was found with molybdate anion.

Table 16. Uranium Competition Studies with Phosphonate Ester SAMMS

Competitor	Concentration	Kd (U) Ac-Phos diethyl ester	Kd (U) Prop-Phos diethyl ester
None		12238	210
Fe(III)	100 ppm	1619	64
Al(III)	100 ppm	10856	206
Zr(IV)	100 ppm	13375	120
Ni(II)	100 ppm	10523	572
Ca(II)	100 ppm	14701	452
Mn(II)	100 ppm	13079	254
Mo(VI)	100 ppm	9660	80
Cu(II)	100 ppm	12300	407
Pb(II)	100 ppm	16128	204
Cr(III)	100 ppm	11969	214
Hg(II)	100 ppm	15857	147
Phosphate	0.01M	11857	246
Sulfate	0.01M	12066	318
EDTA	0.01M	14236	345
Citrate	0.01M	13444	313

[U] = 2000 cpm/mL
1M $NaNO_3$
0.1 M HNO_3
0.10 g SAMMS in 10 mL

In contrast to the esters, the phosphonic acid SAMMS show no interference whatsoever from either competing transition metal cations or complexants (Table 17). The Pu (IV) binding affinity remains high in the presence of a wide variety of competitors. It should be noted that these kinetics were carried out with high nitrate concentrations, revealing that the phosphonic acid SAMMS can compete with nitrate, as well as EDTA, very effectively.

Table 17. Pu (IV) Competition Studies Using Phosphonic Acid SAMMS

Competitor	Concentration	Kd (Pu) Ac-Phos	Kd (Pu) Prop-Phos
		acid form	acid form
None		21206	15844
Fe(III)	100 ppm	21210	14425
Al(III)	100 ppm	28770	10733
Zr(IV)	100 ppm	20483	15877
Ni(II)	100 ppm	20477	16387
Ca(II)	100 ppm	19622	15945
Mn(II)	100 ppm	17762	15999
Mo(VI)	100 ppm	18933	13124
Cu(II)	100 ppm	18846	16415
Pb(II)	100 ppm	19940	17530
Cr(III)	100 ppm	18319	14997
Hg(II)	100 ppm	16281	15844
Phosphate	0.01M	20406	17547
Sulfate	0.01M	19847	18236
EDTA	0.01M	20459	15579
Citrate	0.01M	23116	18655

[Pu] = 2000 cpm/mL
1M NaNO3
0.1 M HNO3
0.10 g SAMMS in 10 mL

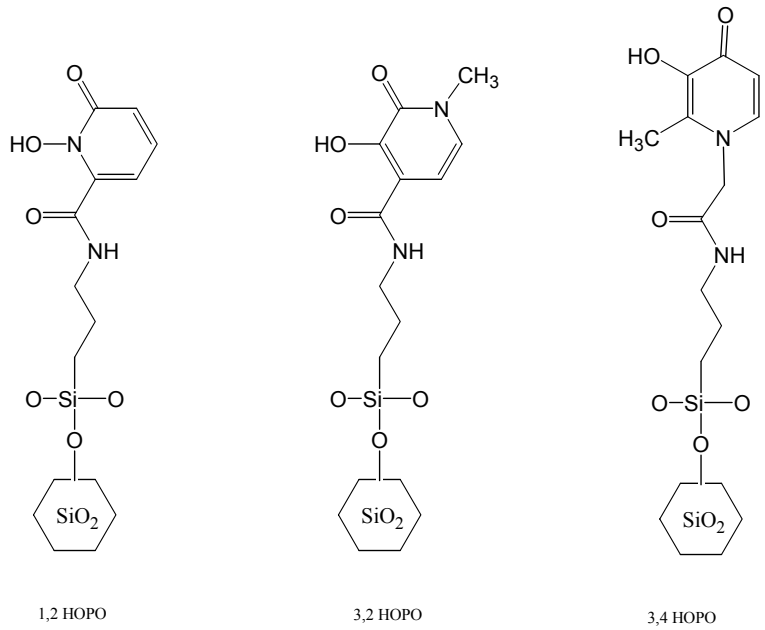

1,2 HOPO 3,2 HOPO 3,4 HOPO

Figure 10. Ligands Used in HOPO SAMMS

HOPO SAMMS. The HOPO ligands developed by the Raymond group at Berkeley are among the finest Pu ligands ever developed [11]. We obtained samples of these ligands and incorporated them into SAMMS using the CDI and thiaz activation routes described earlier. Both the 1,2 HOPO and 3,2 HOPO SAMMS were found to provide exceptional affinity for Pu(IV), although the 3,2 HOPO ligand does seem to show some pH and nitrate dependence.

Table 18. Pu (IV) Distribution Coefficient Studies Using HOPO SAMMS

SAMMS	Solution	Kd (Pu)
1,2-HOPO	0.1M NaNO3/0.1MHNO3	356,000
	0.1M NaNO3/pH=2.0	349,000
3,4-HOPO	0.1M NaNO3/0.1MHNO3	43,500
	0.1M NaNO3/pH=2.0	17,500
3,2-HOPO	0.1M NaNO3/0.1MHNO3	37,000
	0.1M NaNO3/pH=2.0	350,000

initial [Pu] = 2000 cpm/mL
6 mL solution, 30 mg SAMMS

Preliminary experimentation revealed that not only are these ligands particularly good at sequestering Pu (IV), but also Np (V), which is particularly mobile and difficult to sequester, and therefore a particularly important environmental target. Clearly HOPO SAMMS are superior to the other ion exchange materials and represent a major step forward for the sequestration of Np (V), and so we focused our efforts on characterizing the binding of Np (V) by these materials. Clearly, 3,2 HOPO is the best sorbent material for sequestering Np (V), followed by the Prop-Phos acid SAMMS.

Table 19. Np (V) Distribution Coefficients Using Different SAMMS in Groundwater and Glass Leachate Matrices

Hanford groundwater matrix Np-237	
SAMMS	**Kd (Np)**
1,2 HOPO	15,000
3,2 HOPO	152000
3,4 HOPO	4730
Prop-Phos (ester)	53400
Prop-Phos (acid)	20500
Ac-Phos (ester)	8710
Glass leachate matrix Np-237	
SAMMS	**Kd (Np)**
1,2 HOPO	2870
3,2 HOPO	127000
3,4 HOPO	1430
Prop-Phos (ester)	1710
Prop-Phos (acid)	19700

solution/solids ca. 1000

As might be expected, the weakest of the HOPO ligands, the 3,4 HOPO, was found to experience the greatest number of competitive interactions. Its binding affinity was attenuated in the presence of ferric ion, Zr (IV), molybdate and sulfate anions. However, both the 1,2 HOPO and 3,2 HOPO SAMMS were found to be relatively insensitive to the presence of competing species (the notable exception being Zr(IV), which has a severe impact on the 1,2 HOPO SAMMS binding affinity). Clearly, the 3,2 HOPO moiety is a very effective Pu ligand interface within a mesoporous matrix.

Table 20. Pu (IV) Competition Experiments Using HOPO SAMMS

		Kd (Pu)	Kd (Pu)	Kd (Pu)
Competitor	**Concentration**	**1,2 HOPO**	**3,4 HOPO**	**3,2 HOPO**
none	100 ppm	83,700	4,250	41,900
Fe(III)	100 ppm	17,800	495	30,700
Al(III)	100 ppm	28,400	5,370	27,700
Zr(IV)	100 ppm	417	63	47,300
Ni(II)	100 ppm	83,400	4,420	46,000
Ca(II)	100 ppm	96,100	4,380	42,900
Mn(II)	100 ppm	84,000	4,710	46,500
Mo(VII)	100 ppm	29,000	0	39,600
Cu(II)	100 ppm	30,200	4,710	38,700
Pb(II)	100 ppm	84,700	3,980	50,400
Cr(III)	100 ppm	75,900	4,380	43,100
Hg(II)	100 ppm	61,300	2,580	55,600
phosphate	0.01M	129,000	2,880	48,300
sulfate	0.01M	85,900	128	53,200
EDTA	0.01M	188,000	2,960	60,000
citrate	0.01M	180,000	1,480	58,300

Pu (IV) 2000 dpm/mL, 1M $NaNO_3$-0.1M HNO_3, 0.03g SAMMS, 6.0 mL

Note that the data in Table 20 was carried out using 1 M NaNO3 (as opposed to the 0.1M NaNO3 used in Table 18). The lower values in Table 20 are a reflection of the nitrate competition described earlier. Unfortunately, the limited HOPO ligand supply precluded detailed studies of nitrate dependence or sorption kinetics.

Anions SAMMS

The development of effective anion binding materials is a very active field of research. A wide range of anion exchange resins (based on ammonium ion exchange sites), and inorganic adsorbing materials (alumina, phosphate, and zeolytic materials) have been used, but their selectivity and capacity are orders magnitude behind the performance of typical cation adsorbing materials. The ability to selectively sequester pertechnetate from complex mixtures or groundwater is a highly desirable goal, and one that would expedite the DOE clean-up effort tremendously. Therefore we chose to apply the SAMMS concept towards the selective sequestration of tetrahedral oxometallate anions, such as pertechnetate. We used chromate as a model system for most of these studies.

Making SAMMS a suitable anion exchange material was accomplished by lining the mesopores with cationic metals complexes. We specifically targeted those complexes that would

allow for a direct interaction between the cationic receptor and the target anion. In addition, we selected a complex geometry that would allow for a stereospecific interaction between the ion pair. The classical octahedral metal complex presents an almost ideal template for the binding of anions containing C_3 symmetry (an important subgroup of T_d symmetry). Three *fac* coordination sites form a quasi-C_3 "basket" when viewed from an angle bisecting the three different axes. Filling these coordination sites with amine ligands in essence quaternizes the amines, creating a quasi-C_3 "basket" of quaternary ammonium ions containing hydrogen bond donors in a stereospecific array of suitable dimensions to serves as a host site for a tetrahedral anionic guest. By using silane-tethered ethylenediamines as the amine containing structural subunit, we enhance the binding affinity through chelation and force the octahedral complex into a posture that exposes this C_3 "basket" to the solution interface. In addition, there is also some electropositive character from the central metal cation that "leaks out" around each of the individual ligands. The net result is an electrophilic C_3 symmetry binding site that is stereochemically ideal for the binding of tetrahedral oxyanions.

In this project, we found that metal ethylenediamine (EDA) complexes immobilized on mesoporous silica (M-EDA-Si, where M could be Cu, Ni, *etc*.) to be an extremely efficient anion binding material for chromate. This approach provides for the construction of virtually ideal binding sites for tetrahedral anionic ligands. Nearly quantitative removal of chromate was achieved in the presence of interfering anions for solutions containing up to 100 ppm toxic metal anions under a variety of experimental conditions. These materials also remain effective at even higher anion concentrations (in excess of 1000 ppm). Anion loading of more than 120 mg (anion)/g of adsorption materials was observed. The anion loading capacity of this material is comparable (on a molar basis) to the heavy metal loading capacity achieved with the best cation sorbent materials (functionalized mesoporous silica) reported earlier, when the stoichiometry of binding and the atomic/molecular weight of the target species are taken into consideration. This approach is especially promising considering the rich chemistry that can be explored by subtle variations of the metal complex chemistry.

Representative chromate removal results are shown in Table 21. In all the tests essentially 100 % chromate was removed in a single treatment. The distribution coefficients were found to be significantly in excess of 100,000. Competition experiments with 150 ppm sulfate demonstrated little effect on the binding behavior. Chromate concentrations in excess of 1000 ppm began to saturate the binding sites. The maximum sorption capacity in this system is about 130 mg/g, or 1.12 mmol/g. At a much higher solution to sorbent ratio (500 ml/g), quantitative removal of chromate was observed for chromate levels up to 100 ppm. Higher concentrations of chromate under these conditions resulted in saturation of the Cu-EDA binding sites.

Table 21. Distribution Coefficients of Cu_EDA SAMMS Binding Chromate

[Chromate] initial	Solution/SAMMS	Kd
1 ppm	100	>100,000
10 ppm	100	>100,000
100 ppm	100	>100,000
500 ppm	100	4045
1000 ppm	100	7607
1 ppm	500	>100,000
10 ppm	500	>100,000
100 ppm	500	27,350
500 ppm	500	522

pH ca. 5-6

It should be noted that Cu-EDA SAMMS is also very effective in binding sulfate anions because the sulfate anions are structurally similar to chromate anions and the size difference is not large. When the chromate concentration is low, and there are insufficient chromate ions to cover the binding sites, then there are vacancies in the monolayer interface that the sulfate anion can fill. However, as the concentration of chromate increases and there is sufficient chromate to occupy all the binding sites, the sulfate ions are displaced. For example, at a solution to sorbent ratio of 500 ml/g and 150 ppm sulfate, all ions are adsorbed at chromate concentrations below 100 ppm. When the chromate concentrations are increased to over 100 ppm and the materials approach their saturation capacity, virtually no sulfate is adsorbed. This observation shows that the Cu-EDA-Si materials have a much higher affinity for chromate than sulfate. This conclusion is also supported by the testing results at higher sulfate concentrations: at 1000 ppm sulfate concentration the chromate concentration can be reduced from 27 ppm to 0.8 ppm.

The loading density of the EDA silanes within the mesoporous silica was determined gravimetrically to be 3.3 mmole/g. Assuming a 3 to 1 stoichiometry in the Cu (II) EDA complex, this implies a content of 1.1 mmole of Cu-EDA complex/g sorbent material. This loading density is in excellent agreement with the saturation capacities measured for both chromate and arsenate.

Characterization. TEM analysis of the samples with adsorbed chromate revealed no evidence of massive precipitation of particles containing copper or chromium. Energy dispersive X-ray spectra (EDX spectra) were also collected from the TEM samples. The copper concentration in these samples was roughly 0.15 g Cu/g EDA-SiO_2, similar to that suggested by the weight change during the preparation of Cu-EDA-Si samples. The anion loading is about 20 mg/g for 100 ppm chromate solution, and 131 mg/g for 1000 ppm chromate solution. The EDX results are in excellent agreement with those obtained from the wet chemical analysis.

EXAFS. Analysis of the Cu-EDA chromate adduct using EXAFS revealed that the copper atom was in a trigonal bipyramidal coordination geometry, with the oxometallate anion bound directly to the metal center in a monodentate fashion. The Cu-O bond length was found to be 1.97Å, in addition to 4 Cu-N bonds at 2.01Å each and a Cu-Cr distance of 3.39Å. These results clearly indicate that an EDA ligand has been displaced, thereby allowing a direct interaction between the metal and the anion. Similar results were obtained for arsenate, sulfate and selenate.

Mechanistic Rationale. Ramana *et al*. studied the copper chelated pyridyl and tertiary ammonium polymers for arsenate and selenite binding and suggested that preferred binding of

these anions was due to the solubility difference between the cupric arsenate and other more soluble cupric salts, like chloride and sulfate [13]. This is a reasonable explanation for the high anion binding affinity of our M-EDA-Si materials, however we believe that the M-EDA-Si binding affinity may be initially templated by a more intricate stereospecific coordination process. Ethylenediamine is known to chelate to wide assortment of transition metal cations, and to have a high affinity for cupric ion. The log K_1 for the ethylenediamine and Cu (II) in solution is 10.75, while log K_2 is 9.28 [14]. A third ethylenediamine ligand is known to bind to the cupric ion if present in high enough concentration [15]. The third EDA ligand is known to be weakly held, and the association constant (log K_3) has been determined to be approximately –1 [16]. Since the EDA ligands are a part of a monolayer interface, the local concentration of EDA is quite high and once the Cu (II) ion associates with the EDA ligand, it should be rapidly and tightly incorporated into the monolayer matrix and the high effective interfacial concentration of EDA is expected to facilitate the addition of the third EDA ligand.

Copper (II), being a d^9 species, undergoes Jahn-Teller distortion to alleviate the orbital degeneracy by lengthening the bonds to the two apical ligands. While significant in complexes such as $Cu(H_2O)_6^{2+}$ and $Cu(NH_3)_4(H_2O)_2^{2+}$, this distortion is thought to be minimal in those complexes composed of chelating amines [17]. Thus, the $Cu(EDA)_3$ complex is felt to be approximately octahedral in which the first two EDA ligands are strongly bound and the third is rather labile. We feel that this ligand lability plays a key role in the immobilization of arsenate/chromate. Given that the EDA ligand is weakly bound and therefore easily displaced, and the oxyanion selectivity parallels the solubility of the corresponding copper (II) species, we suggest the following mechanism. The cationic octahedral complex contains an electrophilic basket with C_3 symmetry that forms an ideal host for a tetrahedral anion. Once the anion is coordinated within the C_3 "basket", it "unlocks" the complex, releasing an EDA ligand and binding directly to the cupric ion. In the case of sulfate, the corresponding copper sulfate is soluble, therefore the sulfate ion can dissociate and the unlocking process is reversible. Hence, sulfate can be displaced by an anion that binds more strongly. The analogy of a lock and key is apropos; the adsorption of the anion is like the insertion of a key into its lock, while the displacement of the EDA ligand corresponds the opening of the lock. In the case of sulfate, the key can be removed from the lock after it has been opened. In the case of chromate, since the corresponding copper chromate is insoluble (suggesting that dissociation of the chromate anion is unlikely), therefore once the lock is opened, the key cannot be removed (*i.e.* the unlocking process is irreversible). Molecular modeling studies support this conclusion [18].

In addition, a detailed EXAFS study of the chromate adduct of Cu-EDA SAMMS also supported this mechanism [19]. The results of these studies indicate that two of the amine ligands are displaced from the copper center (from different EDA ligands), the oxometallate anions is bound to the copper ion in a monodentate fashion, and the copper has a trigonal bipyramidal geometry (see Figure 11).

These studies of Cu-EDA SAMMS indicate that SAMMS materials coated with cationic transition metal complexes are a powerful new class of anion exchange materials, and offer great promise for the sequestration of highly mobile, and problematic species like pertechnetate.

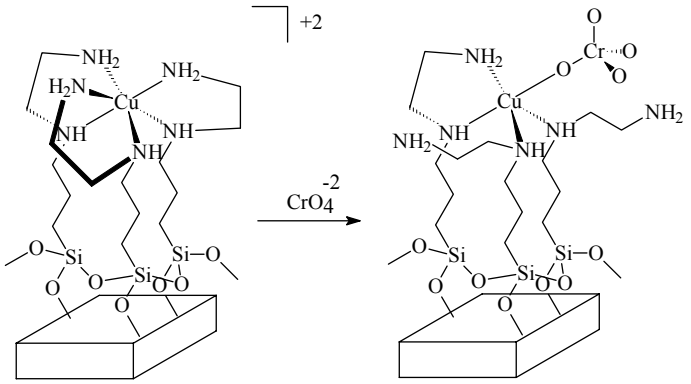

Figure 11. Structure of the Cu-EDA/chromate Adduct

Ferrocyanide SAMMS for Binding Cs

Radiocesium is a significant fraction of the radioactivity of the liquid waste from the reprocessing of nuclear fuel by the Purex Process [20]. The removal of this long-lived radioisotope from fission product waste solution would not only reduce storage problems and simplify ultimate disposal of this waste [20-21], but might also create a possible market for cesium-137 as a commercial source of gamma radiation [22-23]. A number of the older single-shelled tanks are known to be leaking and this has led to the contamination of groundwater around the Hanford area [24]. Therefore, remediation of radiocesium contaminated groundwater is also of great environmental concern. Cesium separation from various solutions has been done for many years principally using ion exchange, solvent extraction, or precipitation processes [25]. Commercial reactors use various natural and synthetic zeolites or cation exchange resins to remove Cs from contaminated water. Precipitation of Cs with tetraphenylborate (TPB) was developed for large-scale Cs removal at the Savannah River Site in the early 1980s. Although the process showed excellent decontamination, decomposition of TPB catalyzed by noble metal fission products led to suspension of work on the process early in 1998. Extensive evaluation of other processes is under way to select a replacement process for TPB precipitation. Work on crystalline silicotitanate (CST) started in 1992 and material was commercially available by 1995. CST has a wide range of applicability from acid to highly alkaline solutions. As a result of the strong adsorption of Cs on CST, all attempts to elute Cs have been unsuccessful. Therefore, CST cannot be regenerated and must be used as a component of the final waste form.

Many different metal ferrocyanides have been prepared and their structure and ion exchange properties have been investigated [26-33]. The advantages of these ion exchangers are their stability in acidic to moderately alkaline medium and their radiation and temperature stability. Furthermore, the affinity series for monovalent ions show preferential cesium sorption for most of the ferrocyanides [27]. Prout and co-workers showed that $K_2CoFe(CN)_6$ was a highly selective ion exchange material with high capacity for Cs [31]. All the products prepared so far by precipitation methods are usually in very fine powders which are difficult to separate from aqueous solutions by filtration. The metal ferrocyanide powders also have too low a permeability to be of any use for column work. Sebesta and co-workers have incorporated KCoFC into the polyacrylonitrile (PAN) matrix to obtain improved column operation [32]. These composite resins also demonstrate rapid kinetics of adsorption. Strelko and co-workers incorporated copper (II) ferrocyanide into vermiculite to sequester radiocesium. These modified

vermiculites showed enhanced affinity for Cs (relative to the parent vermiculite), typically reaching equilibrium in 1-2 hours, with a capacity of 0.05 to 0.13 mmole Cs per gram of sorbent [33].

We extended the SAMMS concept to use ferrocyanide interface to sequester Cs from aqueous solutions. Complete removal of cesium was achieved in the presence of competing metal ions for solutions containing 2 ppm cesium under a variety of conditions. Loading capacity of more than 1.35 mmole cesium per gram of sorbent materials (equivalent to 179 mg/g) has been observed. The fast binding kinetics and high loading capacity (resulting from the extremely high surface area of the support) of the sorbent materials for cesium binding have been demonstrated.

Synthesis and Characterization of FC-SAMMS. Ethylenediamine (EDA) is known to chelate to a wide assortment of transition metal cations, making it very useful as a foundation upon which to build a variety of different metal-ferrocyanide SAMMS. Copper-ferrocyanide was chosen because of its high cesium recovery [34]. In our previous report [18], we used computer modeling to obtain the information of the specific interaction of anions and Cu-EDA-Si material. Based on our previous study, we believe that the octahedral coordination is a good starting point for the Cu-EDA complex on mesoporous silica. The chelating EDA ligand forces the Cu-$(EDA)_3$ complex into a slightly distorted octahedral geometry, the first two EDA ligands being strongly bound and the third being still labile. In the computer modeling, the cationic octahedral complex contains an electrophilic basket with C_3 symmetry that forms an ideal host for an anion, particularly those with C_3 symmetry (or with a C_3 subgroup, such as T_d or O_h symmetry). Once the anion is coordinated within the C_3 "basket," it "unlocks" the complex, releasing (or displacing) an EDA ligand, and binding directly to the cupric ion. The analogy of a lock and key is apropos; the adsorption of the anion is like the insertion of a key into its lock, while the displacement of the EDA ligand corresponds to the opening of the lock. In the case of ferrocyanide anion, it cannot easily dissociate once associated with the copper EDA complex since the corresponding copper-ferrocyanide is insoluble.

The immobilization of copper-ferrocyanide into SAMMS matrix can be summarized in the following reactions:

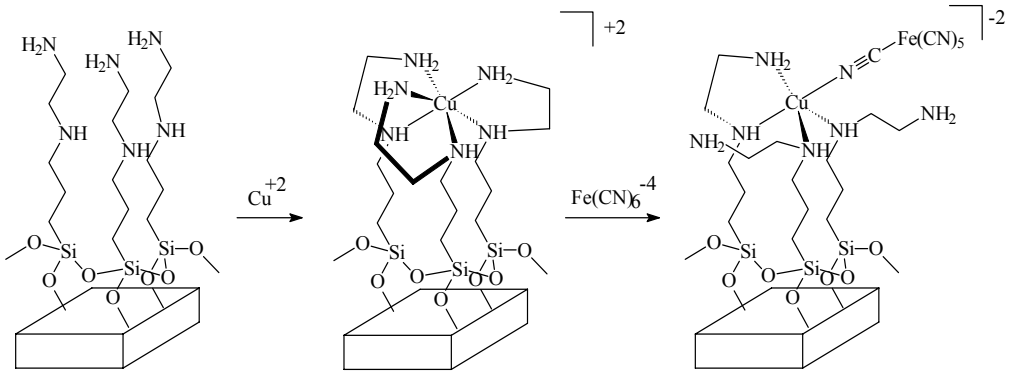

Figure 12. Incorporation of Ferrocyanide anion into the Cu-EDA SAMMS interface

First, Cu (II) ions are bonded to ethylenediamine (EDA) ligands to form octahedral complexes on the surface of the mesoporous silica. Then, ferrocyanide was immobilized on the surface of the mesoporous silica by bonding with Cu.

The surfaces of the Cu-EDA SAMMS materials were investigated with XPS, which clearly showed the nitrogen and copper peaks from the Cu-EDA complex, but no Na or Fe peaks were observed in the original sample. After anionic metathesis, the XPS spectrum of Cu-FC-EDA-SAMMS clearly revealed the presence of both Fe and Na. Depending on the method of preparation, the products of metal ferrocyanides can be non-stoichiometric compounds [35]. Based on these XPS results, the composition of copper ferrocyanide immobilized on SAMMS surface is $Na_{1.3}Cu_{1.5}Fe(CN)_6$. The relative atomic ratios of Na/Cu/Fe were calculated from peak area of Na 1s, Cu $2p_1$, and Fe $2P_3$. When Cu-FC-EDA-SAMMS was saturated with Cs, the Na on the surface of the Cu-FC-EDA-SAMMS was almost completely replaced by Cs. We believe that this is due, in part, to a small amount of ferrocyanide bridging between two adjacent Cu complexes.

Sorption Kinetics and Selectivity. Typical cesium concentrations encountered in these Na bearing wastes is commonly less than 5 ppm [36], so we chose 2 ppm (approximately 1.5 x 10^{-5} mol/L) as being representative for this study. Sorption kinetics play an important role in the efficiency and cost of a sorbent's field deployment. For the 2 ppm cesium solution, Figure 13 shows that Cu-FC-EDA-SAMMS, at a solution to solid ratio of 200 mL/g, reduced the solution Cs concentration to less than 4 ppb within 1 min, and to less than 1 ppb within 2 hours. The cesium sorption kinetics are quite rapid, removing greater than 99% of the Cs in the first minute. These results clearly indicate that diffusion into and out of the mesoporous matrix is not a significant limitation on the overall rate of cesium sorption. Once again, these sorption kinetics are quite similar to those obtained in our previous mercury scavenging studies [3, 6].

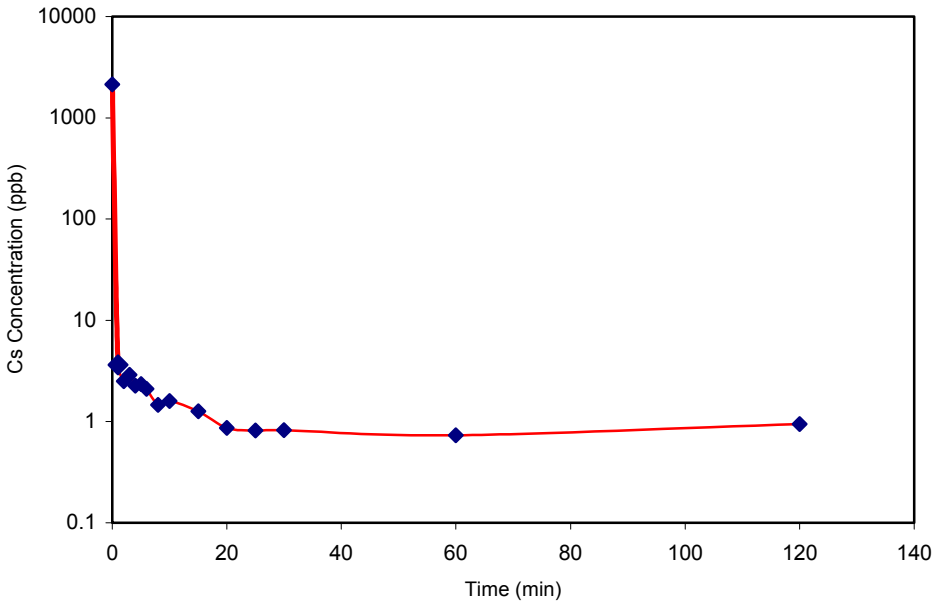

Figure 13. Cesium sorption kinetics by FC-Cu-EDA SAMMS

Since the Cs binding experiments were performed in the presence of a large excess of sodium or potassium, the selectivity of the Cu-FC-EDA-SAMMS for Cs can be inferred from the Cs distribution coefficient (K_d). The major competing ions of metal-ferrocyanide ion exchangers for cesium binding are sodium and potassium. The sequence of affinity of metal-ferrocyanide ion exchangers for three ions is: Na< K<< Cs. In acidic sodium bearing tank waste, sodium and

potassium concentration is 1.41 M and 0.19 M, respectively [36]. To evaluate the selectivity of Cu-FC-EDA-SAMMS for binding of Cs, batch contact experiments were performed at various concentration of sodium and potassium. Table 22 shows that the Cu-FC-EDA-SAMMS has very high selectivity for Cs even at high concentration of sodium and potassium from both neutral and acidic solutions. In all the tests essentially 100% Cs was removed in a single treatment. The residual concentration of cesium is below the detection limit of ICP-MS (Detection limit for Cs is 4 ppb at high salt concentrations). The distribution coefficients were found to be significantly in excess of 100,000 mL/g.

Table 22. Cs Binding in the Presence of Competing Cations

Sample	[Cs] (ppb)	[Cs] (ppb)	Kd (Cs)
3M NaNO3 + 1M HNO3	2170	<4	>108,000
3M NaNO3	2100	<4	>105,000
1M NaNO3	2140	<4	>107,000
0.1M NaNO3	2150	<4	>107,000
0.01M NaNO3	2120	<4	>106,000
1M KNO3	2230	<4	>111000
0.1M KNO3	2210	<4	>110000
0.01M KNO3	2190	<4	>110,000

10 mL solution, 0.05g SAMMS

Sorption Isotherm. The equilibrium cesium loading depends on the cesium concentration in the liquid phase. The Cs adsorption in 0.1 M HNO_3/0.1 M $NaNO_3$ solutions exhibited Langmuirian adsorption and showed an excellent fit (R^2 =0.997) to the Langmuir isotherm equation, which follows the general form:

$$C_f/Q = 1/Kb + C_f/b$$

where C_f is the equilibrium concentration of Cs (mg/L), Q is the amount of Cs adsorbed on the SAMMS surface (mg/g), K is the Langmuir adsorption constant (L/mg), and b is the maximum amount of Cs (mg/g) that can be sorbed by the SAMMS. Fitting the data and solving for K and b yielded values of 0.197 L/g for K and 179 mg/g for b. The excellent fit of a Langmuir isotherm curve suggests monolayer adsorption of Cs onto the SAMMS interface. Clearly, a "perfect" monolayer of Cs is unlikely given the chemical structure of the SAMMS interface, but the agreement of the experimental data with the Langmuirian model supports the conclusion that the ferrocyanide and cesium are uniformly distributed throughout the pore surfaces. The maximum loading of 179 mg/g determined from the Langmuir isotherm equation is also in excellent agreement with the experimentally observed maximum loading of 177 mg/g (1.33 mmole/g), lending further support for the proposed structure and mechanism.

Cesium Capacity. XPS analysis revealed that the Cs/Fe ratio in the Cs laden SAMMS was 1.4, which is quite similar to the starting Na/Fe ratio, supporting a simple cation metathesis mechanism. This observation can be correlated to overall cesium capacity by the following considerations.

Solid-state ^{29}Si NMR indicated a monolayer composed of 4.9 silanes/nm^2. This is the equivalent of approximately 3.2 mmoles of EDA silane per gram of SAMMS. Assuming a 3:1 stoichiometry between the EDA ligands and Cu (II) ion, this indicates a Cu (II) loading of 1.1

mmole/g SAMMS. XPS analysis revealed a Cu/Fe ratio of 1.5 (vida supra), indicating incomplete incorporation of ferrocyanide into the Cu-EDA monolayer interface. Thus, there are approximately 0.74 mmole of ferrocyanide per gram of SAMMS, which would indicate a theoretical cesium capacity of 1.5 mmole Cs per gram of SAMMS based on a projected 2:1 Cs/Fe stoichiometry. XPS analysis of the original (i.e. Na laden Fc-Cu-EDA SAMMS) indicated a Na/Fe ratio of only 1.3 indicating that only part of the ferrocyanide's negative charge is charge-balanced by Na cations, suggesting that a fraction (roughly one third) of the ferrocyanide anions are bridging between two Cu-EDA complexes (this bridging is likely responsible for the incomplete ferrocyanide incorporation). Thus, correcting for ferrocyanide bridging allows one to predict that the Fc-Cu-EDA SAMMS should have a Cs capacity of approximately 1.0 mmole/g. Note that the experimentally determined cesium capacity (1.33 mmole/g) is nicely bounded by the predictions based on ferrocyanide content (1.5 mmole/g), and the value predicted by noting the reduced sodium content and correcting for ferrocyanide bridging (1.0 mmole/g). Whether or not this sort of ferrocyanide bridge can be cleaved via complexation with cesium is unknown at this point.

The Q4/Q3 ratio (i.e. the ratio of quaternary to tertiary silica units) of MCM-41 varies somewhat, but roughly one third of the silicon atoms of MCM-41 are hydroxylated and a Q4/Q3 ratio of 2 can be taken as representative. Assuming that one third of the SiO_2 units in the starting MCM-41 are on the surface and available to anchor a silane molecule, and two thirds are buried beneath the surface then the "molecular weight" of that basic unit (i.e. 3 EDA silanes, 9 SiO_2s, one copper, one ferrocyanide and two cesiums) comes to 1518 g/mole. Since that basic unit binds 2 equivalents of cesium, that leads to a predicted cesium capacity of 1.3 mmole/g SAMMS. The excellent agreement found between this simple model and prediction, and the experimentally determined capacity (1.33 mmole/g) once again lends support to the proposed structure and mechanism.

Adsorbed Cs can be stripped from the Cs-specific SAMMS by a solution which contains an oxidation reagent. This step involves the oxidation of Fe (II) to Fe (III):

$$\text{Cs-Cu-FC-EDA-SAMMS} \text{ -------}\rightarrow \text{Cu-FC-EDA-SAMMS} + Cs^{+} \qquad (5)$$

Elution solutions containing oxidation reagents which oxidize Fe (II) to Fe (III) can be used for stripping of Cs. It was demonstrated that 6-8 M nitric acid solutions can elute cesium from KCoFC incorporated into the polyacrylonitrile (PAN) matrix [32].

Regeneration of the Cs-Specific SAMMS involves the reduction of Fe (III) back to Fe (II). Hydrazine has been demonstrated to be an effective reducing agent for regeneration of KcuFC [37]. Other reducing agents which can reduce Fe (III) to Fe (II) can also be used.

Supercritical Fluid (SCF) Methodology

The use of supercritical carbon dioxide ($SCCO_2$) as the reaction medium for the deposition of self-assembled monolayers in mesoporous ceramics was found to provide significantly enhanced silanation kinetics, unprecedented degrees of surface coverage, and the highest monolayer quality reported to date. $SCCO_2$ provides a very fast, effective, and efficient method for derivatizing a range of porous materials.

Supercritical fluids (SCFs) have been used as low viscosity, low surface tension reaction media in which kinetic rate enhancements are frequently observed [38]. The source of these kinetic enhancements varies from reaction to reaction, but they have been attributed to such phenomena as enhanced mass transfer, a change in local dielectric constant, or enhanced solute-

solute interactions (or reactant aggregation) [38]. High pressure has also been found to increase the reaction rate of associative processes [39-40]. High pressure chemistry has been used in the synthesis of complex molecules where traditional thermal methods failed or damaged the products [41]. The low viscosity and high diffusivity inherent to SCFs are ideally suited for rapid transport of reagents into a nanostructured ceramic phase. Siloxanes are known to be very soluble in supercritical carbon dioxide ($SCCO_2$) [42], making this a logical candidate for reaction medium for the high-pressure deposition of siloxane-based monolayers within a mesoporous framework.

It is well beyond the scope of this report to fully describe criticality and its consequences. However, a brief description of the phenomenon as it pertains to the functionalization of surfaces in small pores may prove useful. Densities similar to that of liquid phases are achievable with a supercritical fluid, given high enough pressures. This allows the fluid to "shield" solute molecules from each other approximately as well as a liquid solvent. However, the elevated temperature prevents the molecules of the supercritical fluid from interacting attractively enough to form long-lived structures, resulting in diffusivities and viscosities similar to those of a gas. The combination of these properties makes supercritical fluids very useful solvents. In particular, supercritical fluids permeate and penetrate small orifices readily.

The kinetics of traditional solution-phase synthesis of SAMMS are restricted by the mass transport of the silane to the inner pore surfaces. This mass transport term is affected by the interfacial wettability of the solvent/silica system, solvent bilayer shear forces, and bulk solvent viscosity. Use of a supercritical fluid as the reaction medium takes advantage of the liquid-like solvating properties and gas-like physical properties of supercritical fluids. Carbon dioxide is an attractive solvent because it is environmentally benign, non-toxic, non-flammable, and inexpensive; the mild critical point conditions for CO_2 ($T_c = 31.1°C$, $P_c = 73.8$ bar) are easily attained and are unlikely to cause degradation of either the mesoporous starting material or the SAMMS product. In addition, performing the silanation in $SCCO_2$ also enhances delivery of the silane to the internal pore surface by direct pressure pumping.

We chose mercaptopropyltrimethoxysilane (MPTMS) as our baseline model system in the development of novel synthetic methods since thiol-SAMMS have proven to be extremely effective in the sequestration of heavy metals [1-7], as well as providing key precursors to nanostructured materials with sulfonic acid functionality [43-44].

In a hypothetical associative reaction between reagents A and B, increasing pressure can increase reaction rate (an excellent, detailed treatment of this subject is provided by Savage et al. [38]). Both the transition state and the product will have a smaller molar volume than the starting materials. Therefore, both $\Delta v‡$ and $\Delta v°$ will be negative. Thus, increasing pressure will stabilize the transition state relative to the starting materials, thereby lowering the activation energy of the process and increasing the reaction rate, and any equilibrium will be shifted toward the product. Thus, exploitation of $SCCO_2$ as the reaction medium for the synthesis of SAMMS can accelerate monolayer formation both by speeding up delivery of the silanes to the reaction site and by reducing the activation barrier to monolayer formation.

The traditional solution phase deposition of MPTMS, in which the hydrated MCM-41 is boiled in a toluene solution of excess silane for several hours, results in a population density of approximately 3.0-3.5 silanes/nm2. The silane speciation of these materials is approximately 50-60% internal silanes, with the remainder being primarily terminal silanes, with a small fraction of isolated silanes [1, 3]. Use of freshly prepared MCM-41 without the hydration step results in poor surface coverage (approximately 0.5 silanes/nm2) [1]. By following the alkoxysilane

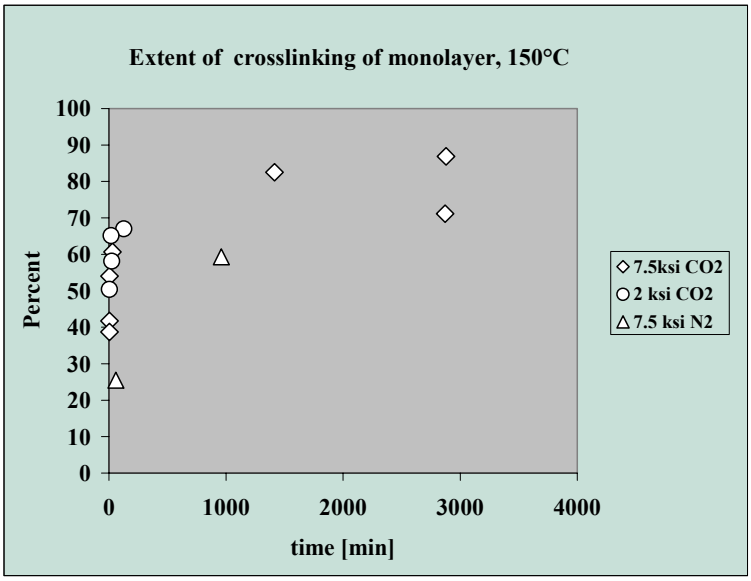

Figure 14. Mole fraction crosslinked silanes as a function of time in the SCF deposition of MPTMS in MCM-41

deposition with an azeotropic removal of the methanol and water by-products, this surface population density can be increased to approximately 4.6 silanes/nm2. The silane speciation of these "azeotropically cured" samples was typically found to be in the range of 60% internal, 40% terminal, and little, if any, isolated silane. Overall, the optimized toluene-phase deposition takes approximately 10 hours of laboratory manipulation time and several days drying time, and

provides decent surface coverage, but still leaves a significant defect density (in the form of dangling hydroxyls, *i.e.* terminal silanes, and pinhole defects).

SCF SAMMS. When the same reaction was carried out under conditions of high pressure (7,500 psi), using $SCCO_2$ as reaction solvent, several notable observations were readily apparent. The deposition chemistry is *much* more rapid (see Figures 14), resulting in complete surface coverage in less than 5 minutes. In addition, the surface population density is noticeably higher (6.5 vs. 4.6 silanes/nm^2) than the toluene solution phase deposition. Following the reaction by ^{29}Si NMR as a function of time, a slow evolution of silane speciation was apparent, with increasing crosslinking as a function of time (see Figures 14). *This is the highest degree of surface coverage and silane crosslinking ever demonstrated for a siloxane-based monolayer.*

One might argue that the gravimetric measurement of the surface coverage is inflated by formation of mercaptopropylsilane polymer in the pores of the material. The NMR spectra of the samples do not indicate the presence of polymer, however. Moreover, as noted above, long term exposure to the $SCCO_2$ resulted in structural degradation of the mesoporous substrate, thereby introducing indeterminacy into the NMR coverage measurements. The speciation measurements are unaffected, however.

In addition, the $SCCO_2$ deposited monolayers were found to display significantly greater stability towards hydroxide ion than do those SAMMS made by the standard toluene procedure (see Figure 15).

The calcined MCM-41 interface is known to be silanol depleted [45]. It is possible that the observed rate enhancement of silane deposition might be attributed to a rapid increase in the surface population of surface silanols, resulting from a pressure-enhanced interfacial hydration

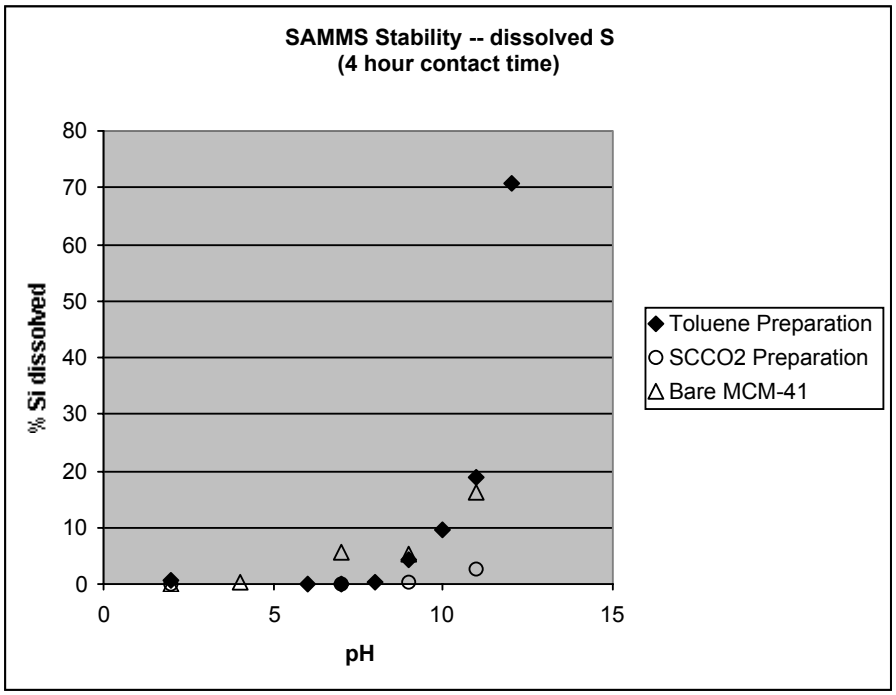

Figure 15. Stability as a function of pH for bare MCM-41, thiol SAMMS made in toluene and thiol SAMMS made in $SCCO_2$.

process. To probe this possibility, control experiments examining siloxane bridge hydrolysis under these conditions were performed. While cleavage of surface siloxane bridges was indeed found to be facilitated slightly by $SCCO_2$ at 7500 psi and 150ºC, the kinetics of $SCCO_2$ hydration were found to be considerably slower than monolayer deposition. Indeed, other work has shown that it is possible to *remove* bulk water from a silica surface by treatment with $SCCO_2$ [46].

Clearly, the enhanced rate of monolayer deposition is not due to the rapid installation of a silanol interface as a result of facile hydration of the silica surface.

In addition, the $SCCO_2$ deposited monolayers were found to display significantly greater stability towards hydroxide ion than do those SAMMS made by the standard toluene procedure (see Figure 15).

The calcined MCM-41 interface is known to be silanol depleted [45]. It is possible that the observed rate enhancement of silane deposition might be attributed to a rapid increase in the surface population of surface silanols, resulting from a pressure-enhanced interfacial hydration process. To probe this possibility, control experiments examining siloxane bridge hydrolysis under these conditions were performed. While cleavage of surface siloxane bridges was indeed found to be facilitated slightly by $SCCO_2$ at 7500 psi and 150ºC, the kinetics of $SCCO_2$ hydration were found to be considerably slower than monolayer deposition. Indeed, other work has shown that it is possible to *remove* bulk water from a silica surface by treatment with $SCCO_2$ [46]. Clearly, the enhanced rate of monolayer deposition is not due to the rapid installation of a silanol interface as a result of facile hydration of the silica surface.

SCFs have been used to prepare porous aerogel ceramics [47], to carry particles and metal clusters into macroporous substrates [48], and to functionalize the interior of zeolites [49]. This project represents the first use of SCFs to prepare fully dense self-assembled monolayer coatings inside a mesoporous matrix. Performing the MPTMS deposition in $SCCO_2$ results in

substantially faster deposition of the silane than when the reaction is carried out in refluxing toluene. A reasonable explanation for the observed rate enhancement can be attributed to the fact that the $SCCO_2$ deposition is carried out at significantly higher pressure than the ambient toluene deposition. An associative process will have a negative $\Delta v^{\ddagger}$ and Δv° (volume of activation and volume of reaction, respectively) associated with it, and increasing the reaction pressure will accelerate such a process, as well as drive any equilibrium towards the adduct (in this case, the monolayer-coated mesoporous ceramic). The formation of a silane-based self-assembled monolayer is the culmination of a complex series of equilibria: silane adsorption, hydrolysis, translocation, condensation, aggregation, and finalized with a series of several additional condensation processes. *Each of these reactions is an associative process and is therefore expected to accelerate with increased reaction pressure.*

The observed rate enhancement might also be attributed to acid catalysis since carbonic acid would be present to some degree due to CO_2/water equilibrium (bulk water in contact with $SCCO_2$ has a pH of approximately 3) [50]. The traditional toluene-phase hydrolysis/condensation chemistry of the monolayer deposition takes place in the acidic environment of a hydrated silica interface (the isoelectric point of hydrated silica is approximately 1.8) [51]. While comparing the exact acidities of these two systems is not possible at this time, it seems reasonable to postulate that their acidities are not hugely different. Supporting the conclusion that the observed rate enhancement is indeed a pressure effect and not due to acid catalysis is the observation that MPS monolayer deposition is almost equally facile from SCN_2 as it is from $SCCO_2$ (See Figure 5 and compare the speciation progress of the sample prepared in SCN_2 with those prepared in $SCCO_2$.) Thus, while general acid catalysis by carbonic acid cannot be ruled out entirely, it is thought to play, at best, a minimal role in the rate enhancement.

MPTMS monolayers prepared in refluxing toluene are typically composed of approximately 3.2 silanes/nm^2 to as much as 4.6 silanes/nm^2. Solid-state ^{29}Si NMR reveals that as many as half of the silanes in these monolayers contain dangling hydroxyls. The increased population density observed in $SCCO_2$ MPTMS depositions can be attributed to a significantly reduced defect density. In a siloxane-based monolayer, there are two primary classes of monolayer defects, pinholes and dangling hydroxyls. The higher surface population is a reflection of the filling in of pinhole defects at higher pressure. The increased crosslinking observed in the longer reaction time $SCCO_2$ depositions is consistent with the Δv arguments outlined above since dangling hydroxyls (which are readily monitored in the ^{29}Si NMR) represent "bumps" and "wrinkles" in the morphology of the monolayer. By carrying out the deposition chemistry out at elevated temperature and pressure, it is possible to "iron out" these wrinkles by facilitating crosslinking, thereby minimizing overall monolayer volume. A reduction in the number of dangling hydroxyls allows the silanes to pack in a somewhat more ordered fashion on the surface, thereby making room for more silanes on the surface. By combining these two defect reduction mechanisms, it is possible to attain higher population densities from $SCCO_2$ than from toluene.

The $SCCO_2$ SAMMS have significantly better stability towards alkaline conditions than do those prepared in toluene. This enhanced stability is simply a reflection of the lower overall defect density. Defects provide access for hydroxide ion to penetrate to the sensitive siloxane anchor beneath the passivating hydrocarbon portion of the monolayer. Both pinholes and dangling hydroxyls provide vulnerability to hydroxide. By enhancing the degree of crosslinking,

and minimizing the pinhole density, the stability of the resulting monolayer towards hydroxide ion is significantly enhanced.

Perhaps the most intriguing observation is the slow evolution of silane speciation as a function of time when exposed to elevated pressure and temperature. This observation is also in accord with the $\Delta\nu$ arguments discussed above and suggests that it is possible for a dangling hydroxyl to "walk" its way through the monolayer until it encounters another, whereupon they undergo condensation thereby annihilating both defects. A control experiment was performed in which the deposition was performed for 5 minutes and then the sample was purged to remove all reaction by-products and then characterized. This sample was then re-subjected to the standard $SCCO_2$ conditions (7500 psi and 150°C) and the same siloxane curing was observed as with those samples that were subjected to the standard $SCCO_2$ treatment. Given the lack of water present during the curing phase of this control experiment, this result also supports the conclusion that it is pressure and not general acid catalysis that is responsible for the enhanced degree of crosslinking in these monolayers.

In addition to the faster deposition chemistry, higher surface population density, higher quality monolayer coverage and greater monolayer stability, other benefits of this $SCCO_2$ protocol include the elimination of the extensive drying period post-deposition and the avoidance of flammable solvents. The waste stream inherent to the toluene preparation is also eliminated since the only by-products of the $SCCO_2$ process are CO_2 and methanol, which are easily separated and recycled.

Aerogel Getter Materials. Aerogels are a cheap, extremely high surface area alternative to the surfactant templated ceramics, the primary difference being that MCM-41 is an ordered hexagonal structure, while aerogels are a random, fractal structure. As an alternative to MCM-41, we explored the deposition of silane-based monolayers within silica aerogels (1250 m2/g). This chemistry is not possible to perform using traditional solution methodology since the capillary forces of the solvent are sufficient to crush the fragile walls of the aerogel support. The aerogel chosen was manufactured by Armstrong, and is a 2 mm. granular solid silica. BET analysis revealed that the pore size distribution of the aerogel is complex, ranging from 200-600 Å. Gentle hydration in SCCO2 caused rearrangement of the pore size distribution to collapse to a uniform pore diameter of approximately 180 Å. More aggressive hydration caused collapse of the aerogel structure, and immersion of the parent aerogel in liquid media crushes the fragile structure of the aerogel due to capillary forces. Deposition of covalently bound monolayers is therefore not possible in traditional condensed phases and is enabled through the use of a supercritical fluid as the reaction medium.

An example of this methodology is provided by the deposition of (ethylenediamino)propyltriethoxysilane (EDAPTMS) in supercritical N_2 (SCN_2). The ^{29}Si NMR spectrum of this material is shown in Figure 16. Note the extremely high degree of crosslinkage, as is evident in the 90%/10% dominance of the –68 ppm. "internal" peak over the –58 ppm. "terminal" peak. *This ability to deposit covalently bound monolayers to the internal surfaces of aerogels is unprecedented, and offers an excellent support for "getter" materials.*

We have furthermore observed that the EDA monolayers laid down from SCN_2 do not suffer from a typical problem encountered in the liquid-based depositions: the amine headgroups have sometimes interacted non-covalently with the silane surface, blocking the formation of a fully dense monolayer. In the SCN_2 deposited materials this behavior is not noted. It is unknown at this time whether that derives from a greater solvation of the amine headgroups by

the SCN_2 or whether the dense monolayer coverage is indicative of the enhanced reaction rates and stabilized intermediate states discussed above.

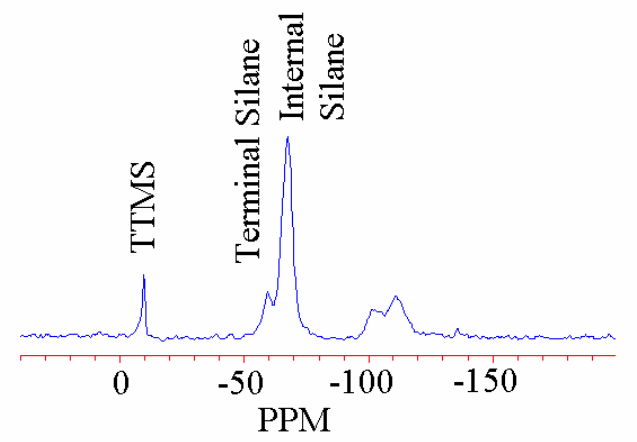

Figure 16. ^{29}Si NMR of EDAPTMS deposited within Armstrong aerogel

CONCLUSIONS

SAMMS is a powerful separation methodology, capable of selectively sequestering actinides and other radionuclides from complex mixtures, even in the presence of large excesses competing ions or complexants. The rigid open pore structure allows for facile diffusion into the mesoporous matrix, providing for fast sequestration kinetics. Self-assembled monolayers terminated in synergistic chelating ligands provide a receptive interface for the binding of lanthanide and actinide cations. The amidophosphonic acid SAMMS and HOPO SAMMS developed in this work have proven themselves as excellent actinide sorbent materials, suffering virtually no competitive interactions with common transition metal cations and/or complexants. Cu-EDA SAMMS represents a powerful new class of anion exchange materials, and appears to have promise as a pertechnetate sorbent material. Ferrocyanide SAMMS are a clearly superior Cs sorbent, with excellent binding affinity and exceptionally fast sorption kinetics. SCF synthetic methodology allows us to make SAMMS much, much faster, and clearly enhances the stability of these hybrid nanomaterials towards alkaline conditions. Being a silica-based separation technology, SAMMS presents the unique capability of being able to selectively extract the radionuclides from tank waste and into a silica matrix, thereby setting the stage to reduce vitrification volume by a factor of approximately 2 orders of magnitude.

RELEVANCE, IMPACT AND TECHNOLOGY TRANSFER

Recently DOE has placed emphasis on the need to significantly reduce the volume of material put through the waste vitrification process. As this project has demonstrated, SAMMS has the ability to selectively sequester actinides and cesium from complex mixtures, offering promise to significantly reduce the volume of waste needing glassification. SAMMS, being a silica-based technology, is completely amenable to vitrification, and could be used to significantly reduce the volume of waste to be glassified since only the volume of the radionuclide-laden SAMMS would have to be vitrified and not the vast bulk of the waste. Due to the tendency of actinides to form insoluble hydroxides and polymeric oxide species at alkaline pHs, *any actinide separation method will require pH adjustment to a pH of less than 4 in order to be viable.* Such pH adjustment will approximately double the waste volume. However, even under the most conservative conditions SAMMS is employed in a solution/solid ratio of 100, *thereby leading ultimately to reducing the volume of waste to be vitrified by a factor of 50!* The likely HLW volume reduction is even greater since SAMMS can be effectively employed at solution/solids ratios of 500 to 1000, and in some cases even higher. As a result of this massive HLW volume reduction, the potential cost savings offered by SAMMS to the DOE clean-up effort is immense.

PROJECT PRODUCTIVITY

This project accomplished everything that it set out in the original proposal. It was hoped that we might also be able to test some of our SAMMS on actual waste, but this proved to be beyond the budget for this project. We were able however to extend the SAMMS radionuclide success beyond the actinides and also do some preliminary and highly promising work with on the sequestration of Cs and TcO4.

PERSONNEL SUPPORTED

Pacific Northwest National Laboratory (PNNL)
Glen E. Fryxell, Tom S. Zemanian, Yuehe Lin, Hong Wu, S.V. Mattigod, Meiling Gong, Jerry Birnbaum

Argonne National Laboratory (ANL)
Kenneth M. Kemner and Shelly Kelly

Lawrence Berkeley National Laboratory (LBNL)
Kenneth N. Raymond and Jide Xu

SAMMS PUBLICATIONS

"Chemistry in Service of Society and the Environment: Toxic Metal Sequestration Using Self-Assembled Monolayers on Mesoporous Supports (SAMMS)" G. E. Fryxell,* S. V. Mattigod, Y. Lin, T. S. Zemanian, H. Wu, J. C. Birnbaum, an invited review for the *Journal of Chemical Education* for their "Products of Chemistry" series (in preparation).

"Actinide Selective Sorbents: Phosphonate Derived Self-Assembled Monolayers on Mesoporous Supports (SAMMS)", Glen E. Fryxell,* Yuehe Lin, Hong Wu, Jerome C. Birnbaum, (in preparation).

"Actinide Selective Sorbents: HOPO SAMMS", Shas V. Mattigod, Yuehe Lin, Glen E. Fryxell,* Jide Xu and Kenneth N. Raymond (in preparation).

"Environmental Applications of Self-Assembled Monolayers on Mesoporous Supports (SAMMS)" Glen E. Fryxell,* Yuehe Lin, Hong Wu, Kenneth M. Kemner, an invited contribution to the Nano3 Conference, to be held in Toronto in June 2002.

"Synthesis of Carbamoylphosphonate Silanes for the Selective Sequestration of Actinides" Jerome C. Birnbaum, Brad Busche, Wendy Shaw and Glen E. Fryxell*, *Chemical Communications* (in press).

"Chemical Functionalization of Nanostructured Materials Using Supercritical Reaction Media", Zemanian, TS, GE Fryxell, J Liu, S Mattigod, Y Shin, JA Franz, O Ustyugov, and Z Nie, Proceedings of the 2001 1st IEEE Conference on Nanotechnology: IEEE-NANO 2001 Maui, HI, Oct. 28-30, 2001.

"Evaluation of Novel Getters for Adsorption of Radioiodine from Groundwater and Waste Glass Leachates" S. V. Mattigod, G. E. Fryxell, R. J. Serne, K. E. Parker, F. M. Mann (submitted to *Radiochimica Acta*).

"Lanthanide Selective Sorbents: Self-Assembled Monolayers on Mesoporous Supports (SAMMS)", Glen E. Fryxell, Hong Wu, Yuehe Lin, Wendy J. Shaw, Jerome C. Birnbaum, John C. Linehan, Zimin Nie, Ken Kemner (submitted to *Chemistry of Materials*).

"Selective Sorption of Cesium Using Self-Assembled Minelayers on Mesoporous Supports (SAMMS)" Yuehe Lin, Glen E. Fryxell, Hong Wu, Mark Englehard, *Environmental Science and Technology* 2001, *35*, 3962-3966.

"Deposition of Self-Assembled Monolayers in Mesoporous Silica from Supercritical Fluids", Tom S. Zemanian, Glen E. Fryxell, Jun Liu, James A. Franz and Zimin Nie, *Langmuir* 2001, *17*, 8172-8177.

"An X-Ray Absorption Fine Structure Spectroscopy Study of the Interactions Between Contaminant Tetrahedral Anions to Self-Assembled Monolayers on Mesoporous Supports" Shelly Kelly, Ken Kemner, Glen E. Fryxell, Jun Liu, Shas V. Mattigod, K. F. Ferris *J. Phys. Chem.* 2001, *105*, 6337-6346.

"X-Ray Absorption Fine Structure Spectroscopy Determination of the Binding Mechanisms of Tetrahedral Anions to Self-Assembled Monolayers on Mesoporous Supports" Shelly Kelly, Ken Kemner, Glen E. Fryxell, Jun Liu and Shas V. Mattigod, *J. Synchtron Rad.* 2000, *8*, 922-924.

"Supercritical Processing of Functionalized Size Selective Microporous Materials" Yongsoon Shin, Thomas S. Zemanian, Glen E. Fryxell, Li-Quong Wang and Jun Liu, *Microporous and Mesoporous Materials* 2000, *37*, 49-56.

"Interfacial Chemistry in Self-Assembled Nanoscale Materials with Structural Ordering" Jun Liu, Glen E. Fryxell, Morris Qian, Li-Quong Wang and Yong Wang, an invited contribution to *Pure and Applied Chemistry* 2000, *72*, 269-279.

"Design and Synthesis of Selective Mesoporous Anion Traps" Glen E. Fryxell, Jun Liu, Meiling Gong, Teresa A. Hauser, Zimin Nie, Richard T. Hallen, Mauxu Qian, and Kim F. Ferris, *Chemistry of Materials*, 1999, *11*, 2148-2154.

"Separation of Complexed Mercury from Aqueous Wastes Using Self-Assembled Mercaptan on Mesoporous Silica", Shas V. Mattigod, Xiangdong Feng, Glen E. Fryxell, Jun Liu, Meiling Gong, *Separation Science and Technology*, 1999, *34*, 2329-2345.

"Investigation of the Local Chemical Interactions Between Hg and Self Assembled Monolayers on Mesoporous Supports" K. Kemner, X. Feng, J. Liu, G. E. Fryxell, L. -Q. Wang, A. Y. Kim, M. Gong, and S. Mattigod, *Journal of Synchrotron Radiation*, 1999, *6*, 633-635.

"Environmental Applications of Self-Assembled Monolayers on Mesoporous Supports (SAMMS)", G. E. Fryxell, J. Liu and S. Mattigod, *Materials Technology*, 1999, *14*, 188-191.

Book Chapters

"Environmental Applications of Interfacially Modified Mesoporous Ceramics" G. E. Fryxell, J. Liu, S.V. Mattigod, L.Q. Wang, M. Gong, T.A. Hauser, Yuehe Lin and K. F. Ferris, and X. Feng; to be published in *Ceramics Transactions*, Volume 107, *Environmental Issues and Waste Management Technologies in the Ceramic and Nuclear Industries,* G. T. Chandler and X. Feng, Eds. pp 29-37, 2000.

"Designing Surface Chemistry in Mesoporous Silica" G. E. Fryxell and Jun Liu an invited contribution to "Adsorption at Silica Surfaces" edited by Eugene Papirer, Marcel Dekker, pp. 665-688, 2000.

"Self-Assembled Monolayers on Mesoporous Supports for Metal Separation" S. Mattigod, G. E. Fryxell, X. Feng and J. Liu in " Metal Separation Technologies Beyond 2000: Integrating Novel Chemistry with Processing", edited by K. C. Liddell and D. J. Chaiko, published by The Minerals, Metals and Materials Society, pp. 71-79, 1999.

"Self-assembled Monolayers on Mesoporous Silica, a Super Sponge for Actinides" X. Feng, L. Rao, T. R. Mohs, J. Xu, Y. Xia, G. E. Fryxell, J. Liu, and K. N. Raymond, *Ceramic Transactions*, Vol. 93*, Environmental Issues and Waste Management Technologies IV,* edited by J. C. Mara and G. T. Chandler, pp. 35-42, 1999. (won the Best Paper Award).

Press Highlights

Chemical and Engineering News (October 15, 2001), "Silica Sorbents with a Taste for Metals" p.32-34.

Popular Science (March 1999), p. 34 "Metal Eaters"

Chemical Engineering (September 1998), p. 17 "Mesoporous Ceramic Sucks up Metals from Solutions"

Process Engineering (September 1998) p. 23, "True Grit Could Help in Clean-Up"

Business Week (September 14, 1998) p. 112, "Researchers Draw a Bead on Toxic Waste"

Hanford Reach (August 24, 1998) p. 4, "Gritty Research Leads Scientists to Metal Loving Discovery"

Industrial Wastewater (July/August 1998) p.24, "Water Technologies Ranked as Top Breakthroughs of Next Decade"

Discover Magazine (July 1998) p. 84, "Sucking Up Mercury"

Environmental Health Perspectives (February 1998) pp. A74-A76, "Quick Fixes for Quicksilver"

INTERACTIONS

Participation/presentations at meetings, workshops, conferences, seminars, etc.

Invited Presentations

"Synthesis of Nanostructured Sorbent Materials Using Supercritical Fluids" G.E. Fryxell, T. S. Zemanian, O. Ustyugov, Y. Shin, Y. Lin, to be presented at the 223rd National Meeting of the American Chemical Society, Orlando, April 2002.

"Selective Sorption of Cesium Using Self-Assembled Monolayers on Mesoporous Supports (SAMMS)" Y Lin,* GE Fryxell, H Wu, and MH Engelhard. An invited talk at Rowland Award Symposium: a symposium to Honor Professor and Nobel Laureate Dr. F. Sherwood Rowland. 222nd ACS National Meeting in Chicago IL, Aug 26-30, 2001.

"Separation and stabilization of radionuclides using self-assembled monolayers on mesoporous supports (SAMMS)", Glen E. Fryxell,* Yuehe Lin, Shas V. Mattigod, Hong Wu, Sandy Fiskum, Tom S. Zemanian, Kenneth Kemner, Jerome C. Birnbaum and Shelly D. Kelly presented as a part of the "U. S. DOE Environmental Management Science Program" co-sponsored by the Nuclear and Environmental Chemistry Sections of the ACS at the 222nd National Meeting of the American Chemical Society, Chicago, August 2001.

"Using Molecular Self-Assembly for Environmental Clean-up Applications", Glen E. Fryxell,* invited contribution to UW Workshop on Nanoscale Science and Technology, Seattle, Aug. 16-17, 2001.

"Selective removal of radionuclides using self-assembled monolayers on mesoporous supports (SAMMS)", Glen E. Fryxell,* Yuehe Lin, Hong Wu, Jerome C. Birnbaum, Tom Zemanian; Invited to contribution to regional ACS Hanford Environmental symposium, NW Regional ACS Meeting, Seattle, June, 2001.

"Selective Sequestration of Lanthanides and Actinides by Self-Assembled Monolayers on Mesoporous Supports (SAMMS), G.E. Fryxell*, Y. Lin, H. Wu, J. C. Birnbaum, W. Shaw, T. S. Zemanian, and J. A. Franz, Battelle, an invited contribution to the Environmental Managed Science Program (EMSP) National Workshop and the Nuclear Materials Focus Area (NMFA), Atlanta, GA, April 2000.

"Actinide-Selective Interfacial Chemistry of Monolayer Coated Mesoporous Ceramics" (poster) G.E. Fryxell*, Y. Lin, H. Wu, J. C. Birnbaum, W. Shaw, T. S. Zemanian, and J. A. Franz, Battelle, an invited contribution to the Environmental Managed Science Program (EMSP) National Workshop, Atlanta, GA, April 2000.

"Self-Assembled Monolayers on Mesoporous Supports (SAMMS) for Lanthanide and Actinide Removal" G. E. Fryxell, Y. Lin,* T. S. Zemanian, Jerome C. Birnbaum, K. N. Raymond and T. R. Mohs, presented as a part of the Actinide Chemistry Workshop sponsored by the Environmental Management Science Program (EMSP) and the Nuclear Materials Focus Area, Albuquerque, New Mexico, Nov. 9-10, 1999.

"Environmental Applications of Self-Assembled Monolayers on Mesoporous Supports" G. E. Fryxell,* T. S. Zemanian, Y. Lin, J. Liu, J. C. Birnbaum, K. Alford, T. A. Hauser, K. F. Ferris, presented as a part of the "First Accomplishments of the U. S. DOE Environmental Management Science Program" at the 218th National Meeting of the American Chemical Society, New Orleans, August 1999.

"X-ray Absorption fine Structure Spectroscopy Determination of the Binding Mechanism of Actinide Surrogate Anions to Self-Assembled Monolayers in Mesoporous Supports" S. D. Kelly, K. M. Kemner,* G. E. Fryxell, J. Liu, T. A. Hauser presented as a part of the "First Accomplishments of the U. S. DOE Environmental Management Science Program" at the 218th National Meeting of the American Chemical Society, New Orleans, August 1999.

"Environmental Applications of Interfacially Modified Mesoporous Ceramics" G. E. Fryxell *, J. Liu, S.V. Mattigod, L.Q. Wang, M. Gong, T.A. Hauser, Yuehe Lin and K. F. Ferris, and X. Feng; presented as a part of Symposium H: Science and Technology Addressing Environmental Issues in the Ceramic Industry; 101st National Meetings of the American Ceramic Society, Indianapolis, April 1999.

"Design and Synthesis of Mesoporous Lanthanide Sorbent Materials" G. E. Fryxell *, J. Liu, M. Gong, S.V. Mattigod, Y. Lin, J. Birnbaum, K. A. Alford, and X. Feng, presented as a part of Symposium G1: Lanthanide Containing Materials and Applications;101st National Meetings of the American Ceramic Society, Indianapolis, April 1999.

"Actinide Specific Interfacial Chemistry on Monolayer Coated Mesoporous Ceramics" Fryxell, G. E.;* Zemanian, T. S.; Kemner, K. M.; Raymond, K. N. invited presentation to the Environmental Managed Science Program/Tank Focus Area Workshop, Richland, WA, Nov. 17-18, 1998.

Presentations

"Chemical Functionalization of Nanostructured Materials Using Supercritical Reaction Media", Zemanian, TS,* GE Fryxell, J Liu, S Mattigod, Y Shin, JA Franz, O Ustyugov, and Z Nie, 2001 1st IEEE Conference on Nanotechnology: IEEE-NANO 2001, Maui, HI, Oct. 28-30, 2001.

"Self-Assembled Monolayers on Mesoporous Supports (SAMMS): A Novel Adsorbent for Removal of Inorganic Contaminants from Water or Waste Streams", S.V. Mattigod,* G. E. Fryxell, R. T. Hallen, K. T. Parker, Second Annual USACE Conference, Severn Trent Laboratories, Louisville, Kentucky, June 5-6, 2001.

"Highly Selective Anion Traps: Self-Assembled Monolayers on Mesoporous Supports (SAMMS)" Shas V. Mattigod, Glen E. Fryxell,* Jun Liu, Richard T. Hallen, Kim F. Ferris, Zimin Nie, Teresa A. Hauser, Meiling Gong, S. D. Kelly, Ken M. Kemner; as a part of the Symposium on Surface and Environmental Chemistry; Combined Rocky Mountain and Pacific Northwest Regional American Chemical Society Meetings, June 17, 2000 in Idaho Falls, ID.

"Self-Assembled Monolayers on Mesoporous Supports: Synthesis of Nanoscale Hybrid Materials and Their Applications", G. E. Fryxell,* J. Liu, T. S. Zemanian, T. A. Hauser, J. A. Franz, K. Alford, K. F. Ferris, L. Q. Wang; presented as a part of the Symposium on Nanoscale Materials at the Northwestern Regional Meeting of the American Chemical Society in Portland, June 1999.

"High Efficiency Environmental Sorbent Materials: Self-Assembled Monolayers on Mesoporous Supports (SAMMS) for Metal Removal from Aqueous Systems", Glen E. Fryxell,* Teresa A. Hauser, Jun Liu, Zimin Nie, Richard T. Hallen, Mauxu Qian, Kim F. Ferris; presented as a part of the Symposium on Environmental Chemistry at the Northwestern Regional Meeting of the American Chemical Society in Portland, June 1999.

TRANSITIONS

MWFA – Removal of Hg from Mixed Waste

TFA – Use of SAMMS as a Semi-Permeable Barrier Technology

DOE-OIT project "Non-Process Element (NPE) Removal Using Functionalized Monolayers on Mesoporous Supports" G. Fryxell,* S. Mattigod, R. L. Leugemors, M. Paster, V. Robinson, D. Biancosino, H. Persinger, AF&PA Headquarters Washington D. C. May 6, **2001**.

NA-22 – Incorporation of SAMMS as a Preconcentration Interface for Enhanced Analytical Sensitivity (Shane Addleman, Tom Zemanian and Glen Fryxell).

Commercialization efforts are currently underway to establish commercial scale capability in SAMMS production.

In addition, an interest (Rocky Flats) for evaluating SAMMS for Pu removal from contaminated oils. There is no existing technology for this remediation.

PATENTS

US Patent #6,326,326 "Surface Functionalized Mesoporous Material and Method of Making Same" (issued Dec. 4, 2001). Two other related patent applications pending.

FUTURE WORK

The fundamental ion exchange capability of SAMMS has been established at this point, but additional selectivity may very well be possible. Areas of research that are clearly needed for deployment of SAMMS in the field include: MCM-41 engineered forms, testing with actual waste, in-situ semi-permeable barriers, use of SAMMS for remote sensing, and in consumer water purification.

LITERATURE CITED

1. "Organic Monolayers on Ordered Mesoporous Supports" Feng, X.; Fryxell, G. E.; Wang, L. Q.; Kim, A. Y.; Liu, J. *Science,* 1997, *276*, 923-926.
2. "Mercury Separation and Immobilization Using Self-Assembled Monolayers on Mesoporous Supports (SAMMS)", X. Chen, X. Feng,* J. Liu, G. E. Fryxell, and M. Gong, Proc. of the 10th Symp. Separation Science and Technology for Energy Applications, October 20-24, 1997, Gatlinburg, TN.
3. "Hybrid Mesoporous Materials with Functionalized Monolayers" Liu, J.*; Feng, X.; Fryxell, G. E.; Wang, L. Q.; Kim, A. Y.; Gong, M. *Advanced Materials*, 1998, *10*, 161-165. (chosen for the cover artwork).
4. "Mercury Separation and Immobilization Using Self-Assembled Monolayers on Mesoporous Supports (SAMMS)", X. Chen, X. Feng,* J. Liu, G. E. Fryxell, and M. Gong, Proc. of the 10th Symp. Separation Science and Technology for Energy Applications, October 20-24, 1997, Gatlinburg, TN.
5. "Investigation of the Local Chemical Interactions Between Hg and Self Assembled Monolayers on Mesoporous Supports" K. Kemner,* X. Feng, J. Liu, G. E. Fryxell, L. -Q. Wang, A. Y. Kim, M. Gong, and S. Mattigod, *Journal of Synchrotron Radiation*, 1999, *6*, 633-635.
6. "Separation of Complexed Mercury from Aqueous Wastes Using Self-Assembled Mercaptan on Mesoporous Silica", Shas V. Mattigod,* Xiangdong Feng, Glen E. Fryxell, Jun Liu, Meiling Gong, *Separation Science and Technology*, 1999, *34*, 2329-2345.
7. "Environmental Applications of Self-Assembled Monolayers on Mesoporous Supports (SAMMS)", G. E. Fryxell,* J. Liu and S. Mattigod, *Materials Technology*, 1999, *14*, 188-191.
8. Cohen, S. M.; Raymond, K. N. *Inorg. Chem*. 2000*, 39,* 3624-3631. Cohen, S. M.; Petoud, S.; Raymond, K. N. *Inorg. Chem*. 1999, *38*, 4522-4529. Cohen, S. M.; Meyer, M.; Raymond, K. N. *J. Am. Chem. Soc*. 1998, *120*, 6277-6286.
9. Caulder, D. L.; Raymond, K. N. *Acct. Chem. Res*. 1999, *32*, 975-982.

10. Rapko, B. M.; McNamara, B. K.; Rogers, R. D.; Lumetta, G. J.; Hay, B. P. *Inorg. Chem*. 1999, *38*, 4585-4592.

11. Xu, Raymond, K. N. *Inorg. Chem*. 1999, *38*, 308-315. Lambert, T. N.; Dasaradhi, L.; Huber, V. J.; Gopalan, A. S. *J. Org. Chem.* 1999, *64*, 6097-6101. Whisenhunt, D. W.; Neu, M. P.; Hou, Z.; Xu, J.; Hoffman, D. C. Raymond, K. N. *Inorg. Chem*. 1996, *35*, 4128-4136.

12. Lambert, T. N.; Jarvinen, G. D.; Gopalen, A. S. *Tet. Lett.* 1999, *40*, 1613-1616. Michael, K. M.; Rizvi, G. H.; Mathur, J. N.; Kapoor, S. C.; Ramanujam, A.; Iyer, R. H. *Talanta* 1997, *44*, 2095-2102.

13. Ramana, A.; Sengupta, A. K. *Environ. Eng*. 1992, *118*, 755.

14. Peters, D. G.; Hayes, J. M.; Hieftje, G. M. in *Chemical Separations and Measurements*; West Washington Square: PA, 1974; p A.12.

15. Gordon, G.; Birdwhistell, R. K. *J. Am. Chem. Soc.* 1959, *81*, 3567.

16. Bjerrum, J.; Nieson, E. J. *Acta Chem. Scand*. 1948, *2*, 297.

17. Plamer, R. A.; Piper, T. S. *Inorg. Chem*. 1966, *5*, 864.

18. "Design and Synthesis of Selective Mesoporous Anion Traps" Glen E. Fryxell, Jun Liu,* Meiling Gong, Teresa A. Hauser, Zimin Nie, Richard T. Hallen, Mauxu Qian, and Kim F. Ferris, *Chemistry of Materials*, 1999, *11*, 2148-2154.

19. "An X-Ray Absorption Fine Structure Spectroscopy Study of the Interactions Between Contaminant Tetrahedral Anions to Self-Assembled Monolayers on Mesoporous Supports" Shelly Kelly,* Ken Kemner, Glen E. Fryxell, Jun Liu, Shas V. Mattigod, K. F. Ferris *J. Phys. Chem.* 2001, *105*, 6337-6346.

20. Northrup, C.J.; Jardine, L.J.; Steindler, M.J. IAEA-SM-261/31, 1983, 461, International Atomic Energy Agency, Vienna.

21. Baetsle, L.H. IAEA-TECDOC-337, 1985, 31, International Atomic Energy Agency, Vienna.

22. Remini, W.C.; Frankhauser, W.A. *Trans.Am.Nucl.Soc*. 1982, *43*, 88.

23. Schulz, W.W.; Bray, L.A. *Sep.Sci.Technol*. 1987, *22*, 191.

24. Sylvester, P.; Clearfield, A. *Solvent Extraction and Exchange*, 1998, *16*, 1527-1539.

25. Thompson, M.C. " Pretreatment/Radionuclide Separations of Cs/Tc from Supernates" Westinghouse Savannah River Company. WSRC-MS-98-00601, 1998.

26. Lee, E.F.T.; Streat, M.; *J. Chem.Tech.Biotechnol*.1983, *33A*, 80.

27. Pekarek, V.; Vesely, U. *Talanta* 1972, *19*, 1245.

28. Ayers, J.B.; Waggoner, W.H. *J. Inorg.Nucl.Chem*. 1971, *33*, 721.

29. Mekhail, F.M.; Benyamin, K. *Radochimica Acta*; 1991, *55*, 95.

30. Ishfag, M.; Karim, H.M.A.; Khan, M.A. *J. Radioanal. Nucl. Chem*., 1993, *170*, 321.

31. Prout, W. E.; Russell, E.R.; Groh,. H.J. J. Inorg. Nucl. Chem. 1965, 27, 473.

32. Sebesta, F.; John, J.; Motl, A. "Phase II Report on Evaluation of PAN as a Binding Polymer for Absorbers used to Treat Liquid Radioactive Wastes." SAND96-1088, Sandia National Laboratory, 1996.

33. Strelko, V. V.; Mardanenko, V. K.; Yatsenko, V. V.; Patrilyak, N. M. *Russ. J. App. Chem*. 1998, *71*, 1746-1749.

34. Valentini, M.T.G.; Stella, R.; Cola, M. *J. Radioanal. Nucl. Chem. Art.* 1986, *102*, 99.

35. Lehto, J.; Haukka, S.; Harjula, R.; Blomberg, M. *J. Chem. Soc. Dalton Trans*. 1990, *3*, 1007-1011.

36. Miller, C. J.; Olsen, A. L.; Johnson, C. K. *Sep. Sci. & Tech.* 1997, *32*, 37-50.

37. Clarke, T.D.; Wai, C.M. *Anal. Chem*. 1998, *70*, 3708-3711.

38. Savage, P. E.; Gopalan, S.; Mizan, T. I.; Martino, C. J.; Brock, E. E. *AIChE Journal*, 1995, *41*, 1723-1778.

39. For reviews of organic reactions under high pressures, see: *Organic Synthesis at High Pressures*, Matsumoto, K.; Acheson, R. M., Eds.; Wiley: New York, 1991. *Organic High Pressure Chemistry*; Le Noble, W. J., Ed.; Elsevier: Amsterdam, 1988. Van Eldik, R.; Asano, T.; le Noble, W. J. *Chem. Rev*. 1989, *89*, 549-688. Isaacs, N. S. *Tetrahedron*, 1991, *47*, 8463-8497.

40. For an excellent summary of how high pressure affects certain kinetic and thermodynamic reaction parameters, see: Diedrich, M. K.; Klarner, F. G. *J. Am. Chem. Soc*. 1998, *120*, 6212-6218. Diedrich, M. K.; Hochstrate, D.; Klarner, F. G.; Zimny, B. *Angew. Chem., Int. Ed. Engl*. 1994, *33*, 1079-1081.

41. For representative examples of the use of high-pressure in the synthesis of complex organic molecules, see: Back, T. G.; Gladstone, P. L.; Parvez, M. *J. Org. Chem*. 1996, *61*, 3806-3814. Kotsuki, H.; Hayashida, K.; Shimanouchi, T.; Nishizawa, H. *J. Org. Chem.* 1996, *61*, 984-990. Araki, Y.; Konoike, T. *J. Org. Chem*. 1997, *62*, 5299-5309.

42. Fink, R.; Hancu, D.; Valentine, R.; Beckman, E. J. *J. Phys. Chem. B* 1999, *103*, 6441-6444.

43. Burkett, S. L.; Sims, S. D.; Mann, S. *Chem. Comm*. 1996,1367-1368. Fowler, C. E.; Burkett, S. L.; Mann, S. *Chem. Comm*. 1997, 1769-1770. Fowler, C. E.; Lebeau, B.; Mann, S. *Chem. Comm*. 1998, 1825-1826.

44. Jones, C. W.; Tsuji, K.; Davis, M. E. *Microporous and Mesoporous Materials*. 1999, *33*, 223-240. Jones, C. W.; Tsuji, K.; Davis, M. E. *Nature* 1998, *393*, 52-54. Van Rhijn, W. M.; De Vos, D. E.; Sels, B. F.; Bossaert, W. D.; Jacobs, P. A. *Chem. Comm*. 1998, 317-318.

45. Cauvel, A.; Brunel, D.; DiRenzo, F.; Garrone, E.; Fubini, B. *Langmuir*, 1997, *13*, 2773-2778.

46. Tripp, C. P.; Combes, J. R. *Langmuir* 1998, *14*, 7348-7352.

47. Loy, D. A.; Russick, E. M.; Yamanaka, S. A.; Baugher, B. M. *Chem. Mat*. 1997, *9*, 2264-2268.

48. Watkins, J. J.; Blackburn, J. M.; McCarthy, T. J. *Chem. Mat*. 1999, *11*, 213-215.

49. "Supercritical Processing of Functionalized Size Selective Microporous Materials" Shin, Y.; Zemanian, T. S.; Fryxell, G. E.; Wang, L. Q. Liu, J. *Microporous and Mesoporous Materials* 2000, *37*, 49-56.

50. Toews, K. L.; Schroll, R. M.; Wai, C. M. *Anal. Chem*. 1995, *67*, 4040-4043.

51. Iler, R. K. *The Chemistry of Silica*; Wiley-Interscience: New York, 1979, p.660.